CHARACTERIZATION OF CARBON-FIBER REINFORCED POLYETHERIMIDE THERMOPLASTIC COMPOSITES USING MECHANICAL AND ULTRASONIC METHODS

by

Mohannad ALHaidri

A Thesis Submitted in

Partial Fulfillment of the

Requirements for the Degree of

Master of Science

in Engineering

at

The University of Wisconsin-Milwaukee

August 2014

ABSTRACT

CHARACTERIZATION OF CARBON FIBER REINFORCED POLYETHERIMIDE THERMOPLASTIC COMPOSITES USING MECHANICAL AND ULTRASONIC METHODS

by
Mohannad ALHaidri

The University of Wisconsin-Milwaukee, 2014
Under the Supervision of Professor Dr. Rani El Hajjar

Continuous fiber-reinforced thermoplastics (CFRT) have the potential for being a mass-produced material for high-performance applications. The primary challenge of using CFRT is achieving fiber wet-out due to the high viscosity of thermoplastics. This results in higher temperatures and pressures required for processing the composites. Co-mingling thermoplastic fibers with a reinforcing fiber, potentially, can enable better wetting by reducing the distance the matrix needs to flow. This could result in shorter cycle times and better consolidation at lower temperatures and pressures. In this study, a polyetherimide (PEI) fiber was comingled with carbon fibers (CF). The resultant fibers were woven into fabrics and processed through a compression-molding technique to form laminates. Control specimens were also fabricated using films of PEI layered between plies of woven carbon-fiber materials. The manufactured CFRT panels were evaluated using ultrasonic C-scans (scans in two spatial dimensions) and then characterized for mechanical properties. The specimens produced using the co-mingled fibers had the cycle time reduced significantly compared to the film CFRT, although the results from the mechanical property evaluations were mixed. The behaviors in the co-mingled laminates can be attributed to the resin- and void-content distribution and the fiber-bundle orientations in the cured composite.

TABLE OF CONTENTS

LIST OF FIGURES

LIST OF TABLES

ACKNOWLEDGMENTS

I would like to thank all of the people who helped in my graduate education. First, I would like to thank Professor Rani Elhajjar, my advisor, for his guidance, support, and his advice throughout my research project. I would also like to thank my committee members, Professor Adeeb Rahman and Professor Benjamin Church, for serving as my committee members and giving some of their valuable time. I also appreciate everyone at the composites lab at the University of Wisconsin—Milwaukee for their time, coaching, and patience, and those who were a great support, especially my lab mate Issam Qamhia for his contribution to the Dynamic Mechanical Analysis section in this thesis.

In addition, I would like to thank the SABIC Innovative Plastics Polymers Processing Development Center members for their support and guidance, particularly Peter Zuber, Ranvir Soni, and everyone else who helped in one way or another. Lastly, my thanks go to my parents, wife, and daughter Tamara for their love, support, and sacrifice through rough times which lead to my success.

Introduction

1.1. Research Problem

Continuous fiber-reinforced thermoplastics (CFRTs) have the potential for being a mass-produced material for high-performance composite applications. CFRTs have several advantages over thermosets-based composites. First, thermoplastics have excellent thermal properties, high toughness, good resistance to some chemicals, and low moisture absorption relative to thermosets. Second, the short cycle times that are possible for thermoplastics make it a good potential alternative because of its significant reductions in manufacturing costs compared to thermosets. However, the CFRT processes are limited by the need for the high temperatures and pressures necessary for quality manufacturing.

Thermosets cannot be re-melted after curing because of the cross-linking reaction in which the polymer chains are connected together, unlike thermoplastics where chains can slide and rotate when the temperature increases. A common method in using thermosets is to use prepreg — layers of semi-cured thermosetting sheets with carbon fiber (CF). This makes it challenging to maintain material stocks due to the limited shelf life of thermoset prepregs which are stored in a refrigerator to slow the curing reaction. In contrast, thermoplastics do not have such a limitation and can be stored for a longer time for off-the-shelf use in manufacturing composite parts. Regarding viscosity, the thermosets' viscosity is much lower than thermoplastics', especially at room temperature, because viscosity in thermoplastics depends on the temperature and shear stress (pressure) applied

to the material. This difference is one of the challenges for commercializing CFRT, although the cycle time for thermoplastics is shorter than thermosets' curing cycle. There is a wide area of research for solutions and simplifications to competitive CFRT production processes, compared with thermoset composites, which are usually time-intensive. Comingled CF/PEI fibers have been selected to be evaluated as a potential method to overcome the viscosity and long cycle-time issues of CFRTs. The comingling process is selected because it will place the PEI fibers in a way that the resin does not need to flow a long distance, helping to reduce the cycle time.

1.2. Research Objectives

One of the alternatives for reducing the cycle times in CFRTs is to use co-mingled thermoplastic fibers. The cycle times are improved by reducing the distance that the matrix needs to flow and thus allow better consolidation. In this research, a polyetherimide (PEI) fiber is combined with carbon fiber fabrics using two methods: carbon fibers with ULTEM® films and carbon fibers comingled with ULTEM® fibers (SABIC Innovative Plastics, Pittsfield, MA, USA). The CFRTs are then processed using a compression-molding technique. The manufactured panels are characterized using ultrasonic C-scans (scans in two spatial dimensions) and resin digestions, and evaluated for their tensile, compression, flexural, and shear properties. The objective of this research is to compare two CF and PEI incorporation methods: plain twill CF weaves with PEI film system and co-mingled fibers in terms of panel preparation methodology, layers handling, and lamination processing time. Furthermore, we will evaluate the panels' quality through non-destructive testing of the mechanical behavior. The study also aims to determine the best methods for characterizing the quality of the CFRTs manufactured using co-mingled fiber composites. In addition, Dynamic Mechanical Analysis (DMA) is used to capture the performance of both co-mingled and film samples for various temperature ranges.

The study is divided into the following sections: 1) flexure properties and material resistance for bending, 2) tension properties for unnotched and notched samples, 3) compression strength under end loading, and 4) shear or interlaminar strength properties. Further, physical testing and optical-microscopic analysis is used to understand the

microstructure of the film- and co-mingled-thermoplastic composite systems and how they relate to the final failure response.

2. LITERATURE REVIEW

2.1. Materials

2.1.1. Fibers

Fiber-reinforced plastics (FRP) consist of fibers and matrix that are bound together physically. The resin transfers the load to the fibers and takes some of the impact and shear stresses and is a major influencing factor in compression and out-of-plane properties. The composite's tension stiffness and strength is dominated by the fiber. Fiber composites can be tailored to suit different applications based on the nature of loading. One of the most common high-performance reinforcements is carbon fiber (CF), which is usually categorized into two types: high-modulus and high-strength. The polyacrylonitrile (PAN) polymer is the origin of high-strength fibers while high-modulus fibers are made from a pitch-based precursor. PAN is influenced by the high polar pendant group with a glass transition temperature at about 80 ^{o}C. However, it starts to degrade before it melts, which is why PAN precursor typically is made by using wet or dry spinning processes. Practically all the commercial PAN precursors are made using the wet-spinning process, where PAN is dissolved in a concentrated polar solvent such as sodium thiocyanate or dimethyl formamide and then extruded through a spinneret to get the precursor. Then, the spun material is oxidized under tension in air at a temperature of

200–270 °C in order to prohibit shrinkage and to avoid polymer chains from relaxing by initiating a cross-linking reaction [1].

Oxidized fibers are then carbonized at temperature between 1000–1500 °C in an inert environment to remove the non-carbon elements. This will result in 55- to 60-percent weight loss. This reduction results in changing the fiber diameter from 35 μm until it reaches approximately 10–12 μm with a high-carbon content. On the other hand, the pitch-based precursor is made using melt-spinning because of it can withstand high temperature without degrading. This helps in having stabilization when the melting point is reached. PAN-based fibers, which are produced by wet-spinning (Figure 1), avoiding high temperatures. Mesophase pitch-based fiber properties are affected by the original process that makes the polymer before spinning, such as catalytic polymerization and solvent-extraction (supercritical fluid) processes. One of these properties is molecular-weight distribution which can either be narrow or wide. This will affect the downstream process for spinning, oxidization, and carbonization [2].

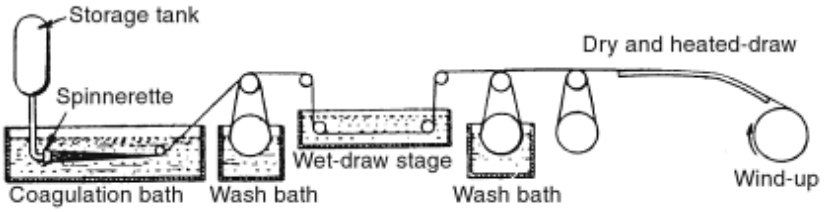

Figure 1. Schematic of a wet-spinning PAN-precursor process to produce fibers [2].

Pitch spinning comes after extruding the pellets through an extruder that will convert the solid to liquid with a rotating screw (Figure 2) and then extrude it through a spinneret. This hot, melted strand is air-quenched during drawdown in order to become solid fibers and collected on the winder. Next is the stabilization process. Unlike the PAN-precursor, pitch-as-spun fibers are highly oriented and thus do not need tension during the oxidation process at 230 to 280 ^{o}C in order to crosslink the polymer chains. Finally, the fibers enter a high-temperature furnace ranging from 1500 to 3000 ^{o}C for carbonization; The weight loss and temperature experienced by the stabilized fibers are important factors in the control of the pitch-based fiber properties [2].

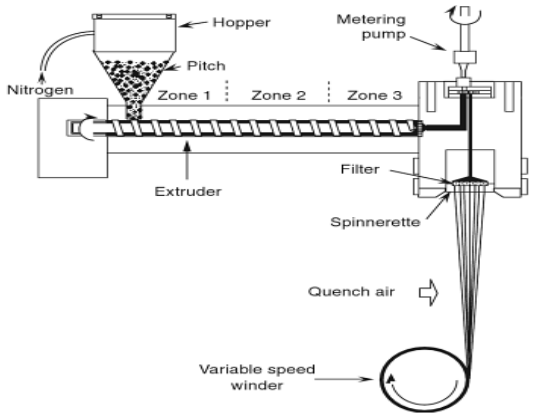

Figure 2. Melt-spinning process for pitch-precursor [2].

In this research the J HTS40 carbon fiber (Tenax, Rockwood, TN, USA) is used to make the samples. The fiber is a high-strength, PAN-precursor that is used for high-

performance composites. The strength of the fiber for the 3K grade is 610 ksi with a modulus of 34.3 Msi with a filament diameter of approximately 7 micrometers [3].

2.1.2. Polyetherimide (PEI)

In polymers, as chain arrangement becomes more random, the polymer becomes amorphous whereas semi-crystalline polymers have aligned chains to form crystal order (Figure 3). Polyetherimide (PEI) is one of the engineering thermoplastics. It is selected because of its superior properties. PEI is an amorphous thermoplastic with excellent thermal properties with the molecular formula of $\underline{C}_{37}\underline{H}_{24}O_6\underline{N}_2$ (Figure 4). The glass transition temperature (T_g) is around 217 ^oC which is on the higher end of plastics. This allows for using the material at high temperatures without losing its mechanical properties.

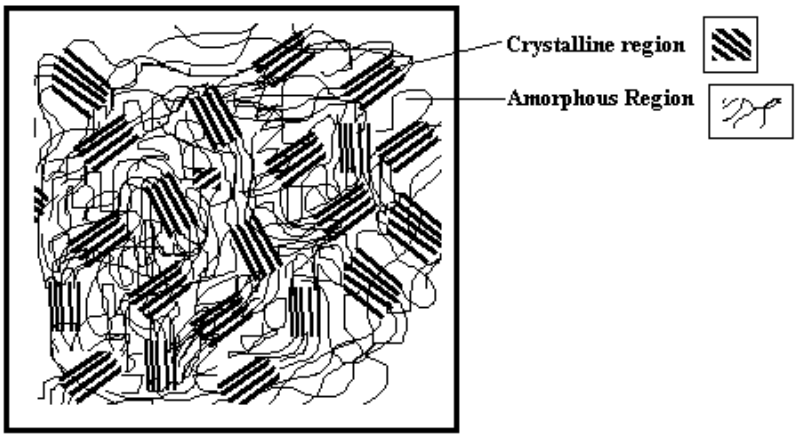

Figure 3. Amorphous and semi-crystalline polymers chain [4].

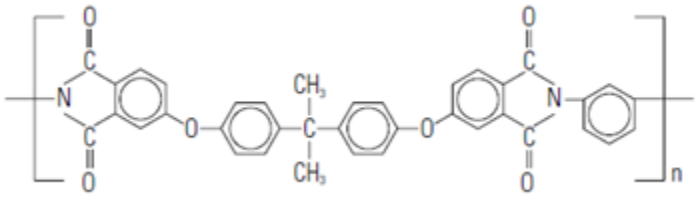

Figure 4. The repeating unit of polyetherimide (PEI).

Dimensional stability and constant performance at higher temperature make PEI an attractive material to be used as a matrix in CFRT. It can be suitable for aerospace, automotive, and other industrial applications. Besides that, PEI has a good flame resistance among other engineering thermoplastics for the resin alone, without adding any flame-retardant additives. However, PEI does not retain its properties when exposed to partially halogenated hydrocarbons and strong alkaline chemicals. ULTEM® 1000 (SABIC Innovative Plastics, Pittsfield, MA, USA) was used for film layers with the following properties: melt flow rate of 9 g/10 min at 337°C, a Poisson's ratio of 0.36, specific gravity of 1.27, tensile stress of 15.95 ksi, and modulus of 519.23 ksi tested at a rate of 5 mm/min [5]. For ULTEM® fibers, grade 9011 was selected as its melt flow rate is 17.8 g/10 min at 337°C, specific gravity of 1.27, tensile stress of 15.95 ksi, and modulus of 519.23 ksi.

2.2. Co-mingled Fiber Systems

Previous researchers have investigated the possibility of co-mingled thermoplastic fibers as an attractive manufacturing technique for fiber composites. This is because of the potential of shorter cycle times and the ability of molding the material to a complex geometry [6]. Co-mingled CFRTs require a high pressure and temperature to be able to impregnate the reinforcement fiber tows due to the high viscosity of the range 500-5000 Pa.s compared to 100 Pa.s for thermoset. Reducing the distance needed for the matrix to flow and at the same time helping in controlling the fiber volume fraction are the main advantages. Benchmarking this process to other processes such as film pre-impregnated have been found to be less flexible than co-mingling, which helps avoid wrinkles while thermoforming [6]. Several attempts were made to characterize co-mingled reinforced fibers with different thermoplastics fibers such as glass with polypropylene fibers (GF/PP), glass with Polyethylene terephthalate (GF/PET), glass with polyamide (GF/PA), glass with polyetherimide (GF/PEI), carbon with Polyether ether ketone fiber (CF/PEEK) and (CF/PA) [7]. Choi have made materials with unidirectional CF co-mingled with polyamide (PA 6) and tested the composites in flexure and found that the interface binding affected the sample strength [8]. It showed higher stress than powder impregnation based composite carried by Friedrich et al [9]. Also, Klinkmüller et al. have studied the effect of the size of the (GF/PP) fiber agglomerations and the pressure-dependent fiber volume fraction in tows using the void content as a measure of quality. It was found that fibers agglomerations affect the cycle time but pressure and temperature had a major influence on the impregnation quality [10]. For tensile properties, Braches

has carried out an experiment to compare carbon fiber, armid, and glass fiber in co-mingled and co-wrapped spun polyamide and Polyetherimide fibers showing that the co-mingled carbon fiber can retain 90% of its strength [11]. Ye reported on the process optimization for compression molding of CF/PEEK co-mingled into a composite (the researchers reported on parameters such as temperatures, holding time, and pressure) and then characterized it using microscopy for void content. The pressure and holding time showed a significant influence on the final composite quality having lower void percentage with good consolidation [12]. Also, flexural tests were conducted in order to assess the product quality and how it was affected by the void content. It was found that the optimum process conditions were a pressing temperature of T = 420 ^{o}C, a compression pressure of 1.5 MPa, and 20 minutes of holding time. Another study by C. Santulli, which focused on the micrograph images analysis for co-mingled GF/PP composites, studied the voids and their influence on the impact properties. The samples were made using two different methods: compression molding and vacuum bag molding with different processing conditions [13]. Ye et al also studied the GF/PP composite microstructure, PP crystallinity and it was found that it can be controlled spherulite crystal. The processing parameters were 200 ^{o}C temperature, 1.5 Mpa pressure and holding time of 20 minutes. Using polarized light microscopy fiber and resin rich region were found having a sharp spherulite boundaries. The investigation showed that slow cooling rate affect the degree of crystallinity starting from 52% up to 70%[14]. For spherulite size, it was found to be smaller near glass fibers while it increases in resin rich region [15]. Also the author investigated the processing conditions of GF/PET and how it

impacted spherulite size which showed no effect, although crystals were found to be smaller than GF diameter. Yet, boundaries were difficult to be recognized. Opposite to GF/PP slow cooling reveled small cracks across the ply [16].

3. Fabrication of Carbon-Fiber Thermoplastic Composites

3.1. Manufacturing Methods

Carbon fiber-reinforced thermoplastic (CFRT) manufacturing is considered a challenge because of the high viscosity of the thermoplastics even at high temperatures and pressures which are known to affect the polymer impregnation. Several methods have been developed to overcome this problem by modifying thermoset processing methods. The main idea in these techniques is to bring the polymer close enough to the fibers and avoid the melting that accompanies moving lengthy distances. The popular methods for impregnating continuous fiber reinforcements in industry are: prepregs, semipregs, powder impregnation, and commingled fibers [17].

Prepregs (Solution impregnation): Prepregs are usually made from amorphous polymers (such as PEI) that are dissolved in a chemical solvent in order to have low viscosity and to impregnate the resin into fabric fibers, like thermosets. Then, the solvent needs to be removed after dispersing the resin in order to make it easier to distribute the

matrix. Next, it is heated to wet out the fibers, then it is cooled down to consolidate the polymer and get the prepreg. Alternatively, a semi-crystalline polymer (e.g. Polyethylene) is used that usually has a high molecular weight (HWM) and thus a relatively good chemical resistance. However, it follows that it has less solubility and cannot distribute the resin like the amorphous plastics (e.g. PEI). Even at high temperatures its viscosity is still high. That makes it difficult to have good consolidation in the prepregs with good quality and less void content. Moreover, there are several disadvantages and challenges in using the solvent process resulting in some weaknesses in the final product. The first side effect is the trace of the solvent that was not removed completely. This leads to degradation in the mechanical and physical properties. Leeser and Banister [18] showed that there is a relationship between the volatiles fraction and the glass transition temperature (T_g). As the percentage of volatiles in the laminates increases, the T_g decreases, thus lowering the service temperature.

Film Staking or Semi-Pregs: Film staking or semi-pregs stack the polymer in the form of thin films between the fiber-fabric layers, and then produces a composite by consolidating them using high temperature and pressure. During the forming process, the film will melt and wets out the fabric. A vacuum is usually used to remove air form the compression compartment in order to eliminate voids. After that, the composite plaques are cooled to lock the resin properties with low voids content [19]. The challenge is to select the right film size in order to avoid having excessive resin. This is one of the challenges that can result in lowering the fibers' volume fraction. Also if the

pressure increases, this will result in squeezing the molten polymer out of the plaques. This makes it difficult to control the resin content, especially on the edges.

Powder Impregnation: Impregnation of the thermoplastic in fine powder form was investigated for use in fabrication of CFRTs. It is performed by spreading the powders in between the reinforcement fibers. After that, layers are placed on top of each other. Heat and pressure is then applied to melt the resin. This results in wetting out of the fibers. The spreading of the powder all over the fabric reduces the distance that the resin needs to flow. A disadvantage of this technique is controlling the particle size of the powder that might lead to damaging the fabric during placing and damaging the fiber orientation thus resulting with a lower-quality panel.

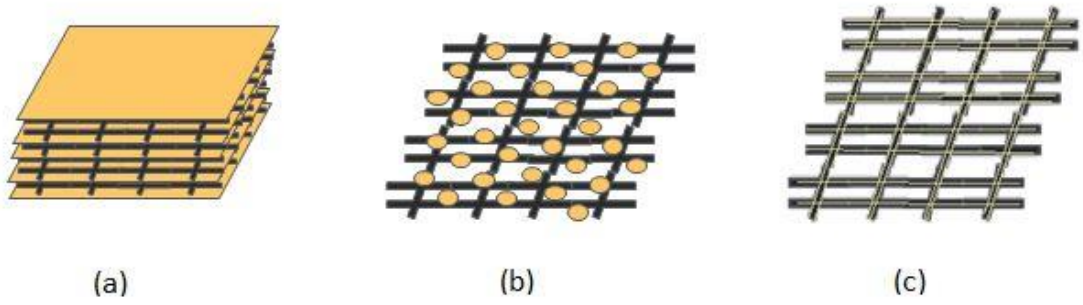

Figure 5. Different types of CFRT processes: a) Film staking, b) Powder impregnation, c) Fibers co-mingling.

Co-mingling or Hybrid fibers/yarns*:* This technique is suitable for polymers with high melt strength and that can also be formed into fibers. Blending the thermoplastic filament with the reinforcement fibers has been accomplished in different ways: co-mingling, co-wrapping, core-spinning, and stretch–broken. First, co-mingling of fibers can be done by having the polymer filament inserted in the reinforcement fiber bundle giving better control of the fiber volume fraction. Then, these comingled fibers are processed further to make woven fabrics. That will be easy to prepare compared to other processes such as film staking and powder impregnation because of yarn twisting. Co-wrapping, on the other hand, is done by wrapping the thermoplastics fibers on the reinforcement fiber tows and adding some protection during secondary processing such as fabric weaving. The disadvantage is that the resin distribution is not well controlled and impregnation is affected. Another point is that higher temperature and pressure are needed in order to overcome the uneven distribution of matrix. A third way of making hybrid fibers is the co-spinning method where the short polymer fibers are spun around the reinforcement's core almost similar to co-wrapping. This makes it more flexible due to the short fibers resulting in further ease of processing conditions compared to other techniques, although it needs further twisting to have better cohesion within the core fibers. The last type is the stretch–broken method which is made by cutting continuous reinforcement and polymer fibers into pieces and then twisting them together into yarns. The advantage of this process is having more flexibility because of the freedom coming from breaking the fibers into a certain length beyond the critical length. However, this

will reduce the tension properties because of incontinence and misalignment of fibers [7].

3.2. Film Panel Fabrication

A lamination press with vacuum assist was used to make the CF/PEI composites. Eight panels were fabricated with 15 layers of carbon-fiber weave and with a size of 8 in. by 8 in. First, the twill weave of carbon fiber fabric roll was placed on the preparation table and 8 in. x 8 in. squares were measured by removing two tows. Then, electrical scissors were used to cut the layers, but before that a tape was used to hold the edges in position during placing and while cutting. After finishing preparing the CF, PEI films with a 5 mil (0.005 inches) thickness were used with smaller dimensions than the CF fabric (7.5 by 7.5 inches) to avoid excessive resin flowing outside the tooling.

Aluminum foil was used to cover the tooling surface in order to avoid the PEI film sticking to the metal surface. A mold release compound (MAC 1031; Maclube, Aston, PA, USA) is also used to make removing the sample easier and to increase the life of the tooling. An important step is curing the mold release in the machine at a high temperature (250 ^{o}F) by putting compound in the tooling with the aluminum foil for 20 minutes. Following this, inserting the shims prevents the molten resin from flowing out of the tooling edges and to maintain the fabric and the PEI films layers in place during processing. The surfaces were cleaned with a piece of fabric, and then a thin layer of MacLube was applied and spread nicely until it covered the whole tool. Next, the CF

weave with the PEI films are placed in an alternating sequence with film layers on the top and bottom (as seen in Figure 5). Care is needed while handling the CF and PEI layers to make sure that small pieces and impurities are not generated during cutting and in the preparation step, in order to avoid defects in panels made. After the collation of the plies, the tool is inserted in the laminating press machine and centered to have equal pressure distribution. The typical process has the plates heated up to 250 ^{o}F with 172 psi pressure (5 tons) under vacuum, followed by increasing the temperature to 650 ^{o}F and then the pressure to 800 psi (20 tons). Finally, the cooling cycle is initiated until the temperature reaches 80 ^{o}F with a rate of 16.67 ^{o}F per minute. A total cycle time of 140 minutes (2 hours and 20 minutes) is used.

Figure 6. Co-mingled CF/PEI weave (left) and a plain carbon-fiber weave (right).

Table 1. Processing conditions for the 8" by 8" film consolidated plaques

Parameters	unit	Plaque No. 3 and 4	Plaque No. 5 to10
1st pressure	ton	4	5
2nd pressure	ton	18	20
1st temperature	^{o}F	350	350
2nd temperature	^{o}F	650	650
3rd temperature	^{o}F	700	700
Holding time	min	15	15
Cooling temperature	^{o}F	80	80
Vacuum	mmHg	26.4	26.4

Table 1 shows the process conditions for the eight plaques that were made with the same conditions. Later on it was decided to make larger plates with the size of 20 by 16 inches based on the ultrasound test results. Table 2 shows the process conditions for the plaques repeated with the same procedure using a bigger fabric and film dimensions. Five plaques were made but this time the shims were not used due to the difficulties while removing them, because of the molten resin's agglutinating effect. Instead, aluminum foils were used and folded at the edges to prevent the resin from flowing, especially with the heavy tooling that is not easy to handle.

Table 2 20" by 16" CF/PEI Film sample's processing conditions

parameters	unit	Plaque No.1, 2 and 3
Pressure	psi	800
Temperature	^{o}F	700
Cooling temperature	^{o}F	80
Vacuum	mmHg	28.6
No. of layers		15
Note		Cycle time 140 mins

3.3. Co-mingled Panel Fabrication

PEI filaments were co-mingled with 3K Tenax®- J HTS40 carbon fibers to form tows with a fiber volume fraction (V_f) of 60% of carbon fibers and 40% of PEI fibers. Textile Engineering and Manufacturing Inc. (Woonsocket, Rhode Island, USA) weaved the comingled tows to make a 2 by 2 twill fabric that was used to make three panels with the size of 20” by 16”. Compared with the CF/PEI film-composite process, the step of cutting the films was eliminated, thus reducing the preparation time. The same procedure was repeated in cutting the CF/PEI co-mingled fabric by measuring the exact dimensions and removing two tows, making it visible and easy to cut with the electrical scissors. Afterwards, aluminum foils were placed on the tooling to avoid surface wrinkling and then white clean fabrics were used to wipe away any particles. A mold-release agent was then spread all over the foils on both sides till it dried and was then placed in the hot plate. Then, 15 layers were stacked carefully to avoid misalignment or particle contamination, the aluminum foils were folded, and the tooling was closed. But before this step, three 8 by 8 inches plaques were made under a fixed pressure with changing temperature to see which one of these was best suited for the co-mingled fabric since there was not much information in the literature. The plaques were cured at 600, 650, and 700 ^{o}F and then tested for flexural strength using the three-point bend test.

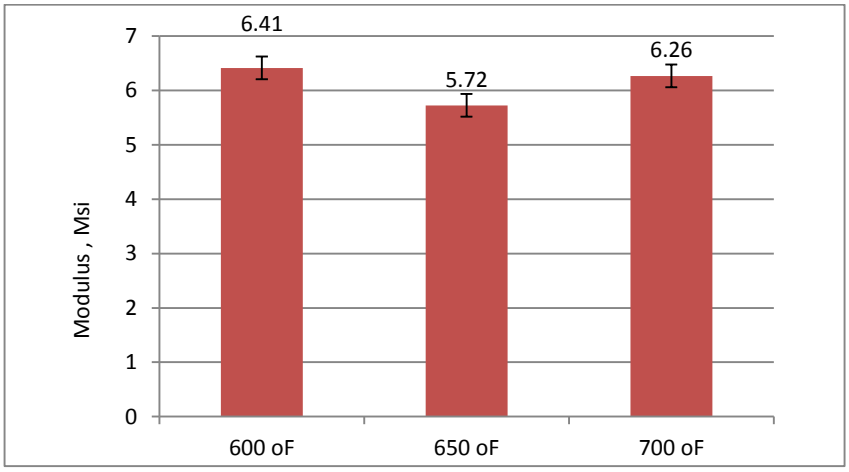

Figure 7. Initial flexural modulus tests on co-mingled panels at three different temperatures.

The three plaques showed that at 600 ^{o}F, with6.41 Msi (an average of 5 samples readings), the modulus was higher than at 650 and 700 ^{o}F, as shown in Figure 7. Based on this outcome, it was decided to go with 600 ^{o}F as the processing temperature for the big plaques. This reduction from 700 to 600 ^{o}F reduced the processing time to 90 minutes and the pressure to 350 psi, as shown in Table 3. The tooling was taken out of the machine for cooling and the aluminum foil was removed from the panels easily.

Table 3. Curing parameters for the 20" by 16" CF/PEI comingled plaques

Parameters		Plaque
Pressure	psi	350
Temperature	^{o}F	600
Cooling temperature	^{o}F	80
Vacuum	mmHg	28.6
No. of layers		15
Note		Cycle time 90 mins

4. NONDESTRUCTIVE CHARACTERIZATION OF TEST PANELS USING ULTRASONICS

Ultrasonic testing (UT) is a non-destructive testing (NDT) method that is commonly used to assess the quality of composite materials. If there is any change in the density or losses due to defects, the speed and amplitude of the sound waves can change and can thus be correlated to the internal quality of the laminate. There are different types of UT testing methods including: pulse-echo, through-transmission, back-scattering and ultrasonic spectroscopy. The focus in this research will be on the through-transmission techniques and comparison to the pulse-echo method. Depending on the geometry and part size, UT can be a contact (manual) or non-contact test where the part is either complex or small and can be immersed in a media tank for better acoustic coupling through water. The composites and the transducer(s) are immersed in the water, which is the most common fluid to conduct the test.

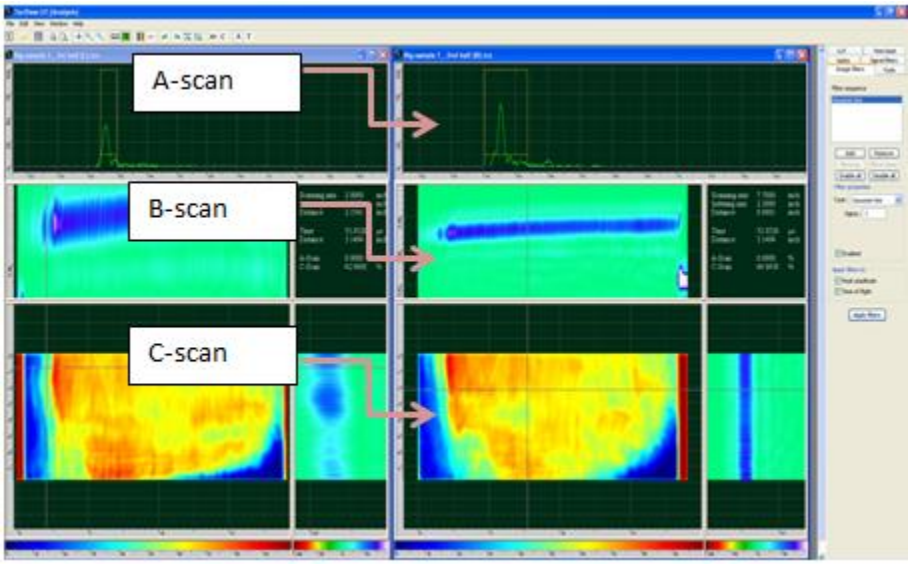

Figure 8. Snap shot from film plaque No.1 UT scanning program for CF/PEI film panel with A-, B-, and C-scans.

4.1. Through-transmission Technique

In the through-transmission UT method, two transducers are used: one acts as the transmitter and the other a receiver [20]. The transducers are held parallel and opposite to each other as shown in Figure 9. The specimen is placed in between the transducers allowing the sound signal to go through the composite layers. The signal intensity is then displayed in the analysis as the percentage of pulse transmission through the composites' thickness. If defects such as porosity are present, the part of the sound pulse will scatter and this will show up as an attenuating region in the C-scan (Figure 8). The main advantage of this technique is that it can scan defects of different sizes, starting form voids and wrinkles up to fiber misplacements and impurities. However, this sensitivity

requires significant calibration and testing to determine the appropriate technique to use. Unlike pulse-echo discussed next, it can detect imperfections at different thicknesses without losing the pulse intensity but it cannot indicate the location of the defect like the pulse-echo method.

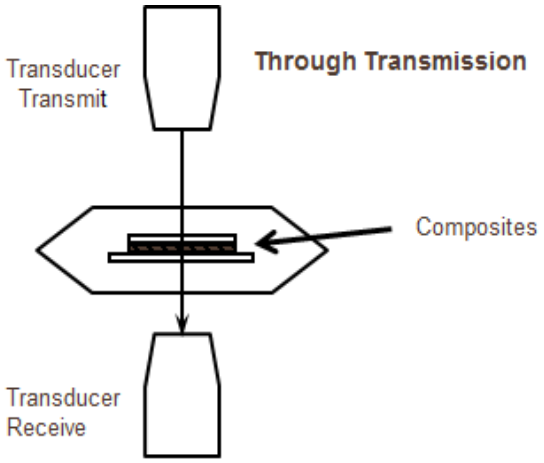

Figure 9. Through-transmission ultrasound testing.

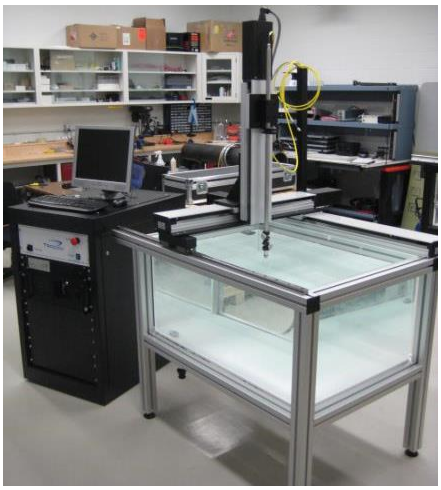

Figure 10. TecScan device equipped with water tank for UT.

In this research, through-transmission UT was used on CF/PEI film and co-mingled composite samples. TecScan (TecScan Systems Inc, Quebec, Canada) equipment was used to carry out the UT scanning with transducers with different frequencies ranging from 1 MHz up to 10 MHz. A specially constructed frame made from PVC pipes was used to hold the panels while scanning under the water. First, the selected frequency transducers were installed (5 MHz in this case), making sure that the sender and receiver were parallel and opposite to each other. Second, the panel was washed and cleaned before immersion in the tank and was wiped slowly to remove air bubbles from both composite surfaces. The panel was positioned in place such that the scanning transducers can cover in the X- and Y-axis. After finding the scanning boundaries on the X, Y, and Z axes, it can be saved in positioned buttons (position 1, 2, and 3) which can be used in moving between the three scanning points. Before starting, one of the important settings was the "received signal gain." This property was selected by manual scanning by moving the scanning head to find the right number that resulted in 70 to 80% of the full-scale signal. From "UT settings" the following parameters were selected: 0.325 in/sec as scanning speed, a scan increment of 0.10 inch, and an index increment of 0.10 inch [21]. The higher speed will affect the resolution and the time needed to carry the scan. To calibrate the transducers, distance pulse-echo mode must be used to center it (the distance is 3.5 inches apart) by moving the frame slowly until the signal reaches the center, which is roughly 1.75 inches to avoid the near field region of the sensor. Finally, a through-transmission mode test was started to scan eight specimens of sizes of 8" by 8" as seen in Figure 11.

Each sample was scanned separately and then in the analysis mode the C-scans were opened together to compare the variation of transmission. Based on these scans it was decided to fabricate bigger panels in order to have homogenous samples for testing. Three panels of 20” by 16” were made. To hold the plaque, the PVC frame was modified and was able to hold half of the plate submerged under water making it possible to require only two scans to complete scanning the panel.

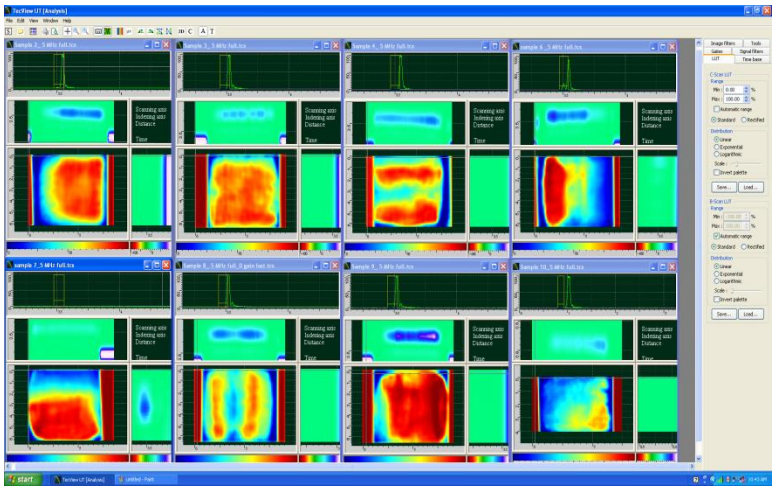

Figure 11. UT scans for eight CF/PEI film samples (8" by 8"). From top left first row: plaque 3, 4, 5, and 6 second row from left: plaque 7, 8, 9, and 10.

The same UT test parameters for the small plaques (8 by 8 inches) were also used for the big plaques. The right part was scanned first and then the left one was completed to cover the entire area. Plaques 1, 2, and 3 were labeled as “F1,” “F2,” and “F3.” In the analysis, the images were filtered and smoothed by applying a Gaussian-blur filter. For the co-mingled plaques, the same scanning parameters were applied first with a 5-MHz transducer but the scan readings came up to be on lower side, indicating a low through-

transmission , so it was decided to use lower frequency. Both transducers were changed from 5 to 1 MHz and the setup was prepared for scanning the three panels “Co-1,” “Co-2,” and “Co-3.”

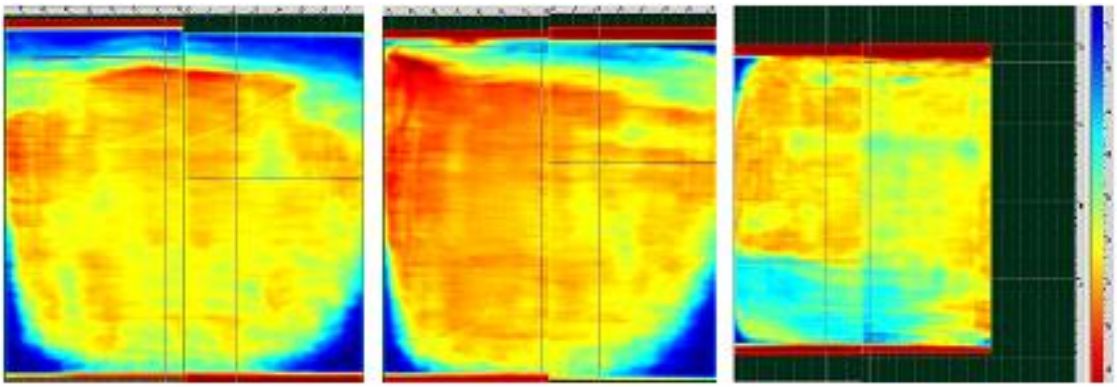

Figure 12. UT scans for three CF/PEI film 20" by 16": a) panel film-1 (left), b) panel film-2 (center), and c) panel film-3 (right).

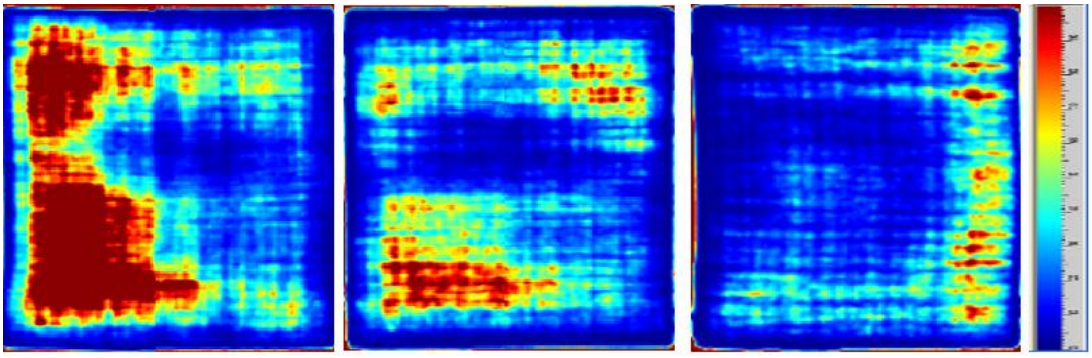

Figure 13. UT scans for three CF/PEI co-mingled 20" by 16": a) panel co-mingled-1 (left), b) panel co-mingled-2 (center), and c) panel co-mingled-3 (right).

Selecting the gain for co-mingled plaques was problematic because of the large fluctuations of panel quality. For example, plaque “Co-1” had a dark red region with high transmission indicated by the colored scale (bottom left area), while on right side of

the plaque a dark blue region representing signal attenuation is seen (Figure 13). After trial and error, a gain of 10, 15, and 20 were selected to have better scan results and it was found that a gain setting of 20 produced good results and covered both ends. Similarly, an image filter was applied to the images (as in Figures 12 & 13) that indicate the regions with high attenuation. These are later compared to the results from acid-digestion tests (discussed in Section 5) in order to verify and relate the scan results with composite density, resin content, and voids percentages.

4.2. Ultrasonic Testing and Manufacturing Defects

Void content is a function of a fabrication and requires careful control in order to reduce its effect on the mechanical properties, as C. Santulli [13] showed in the study of void content in glass/polypropylene co-mingled composites. Yet, the distribution of the matrix filaments in the reinforcement bundles can also play a big role in void content distribution across the plaque thickness. Also, Yang and Elhajjar [22] have shown that porosity content can affect flexural modulus significantly on CF/epoxy at different void contents and sometimes shows increases in flexural modulus at higher porosity. A. C. Long showed an interesting theory about thermoplastic-fiber movement during processing and how it affects the composite microstructure and void content [23]. He proposed that a matrix with large-diameter particles migrate to the surface during the second processes, unlike smaller ones which tend to stay at their locations. The

compression processing parameters — compaction rate, temperature, and pressure on the consolidation of co-mingled glass/polypropylene fabrics — have also been studied [23]. This will affect the co-mingled quality as thermoplastic fiber distribution will be altered resulting in two things: unequal resin formation during consolidation and creation of voids due to fiber migration. These findings align with the results obtained in tests of tension, flexural, compression, and shear strength. However, more research is needed in order to understand the factors that affect co-mingling quality. Therefore, the acid digestion method was used to determine the void and fiber content and to correlate the results with the ultrasonic testing (UT). The UT C-scans showed that there is a large variation in the attenuation in the 8" plaques (No. 3 up to 10). The larger plaques (F-1, F-2, and F-3) showed a more uniform distribution indicating a signal transmission at 70-80% of full scale. When preparing the samples for the mechanical tests, the plaque edges were avoided due to the low transmission that typically correlates to higher porosity levels.

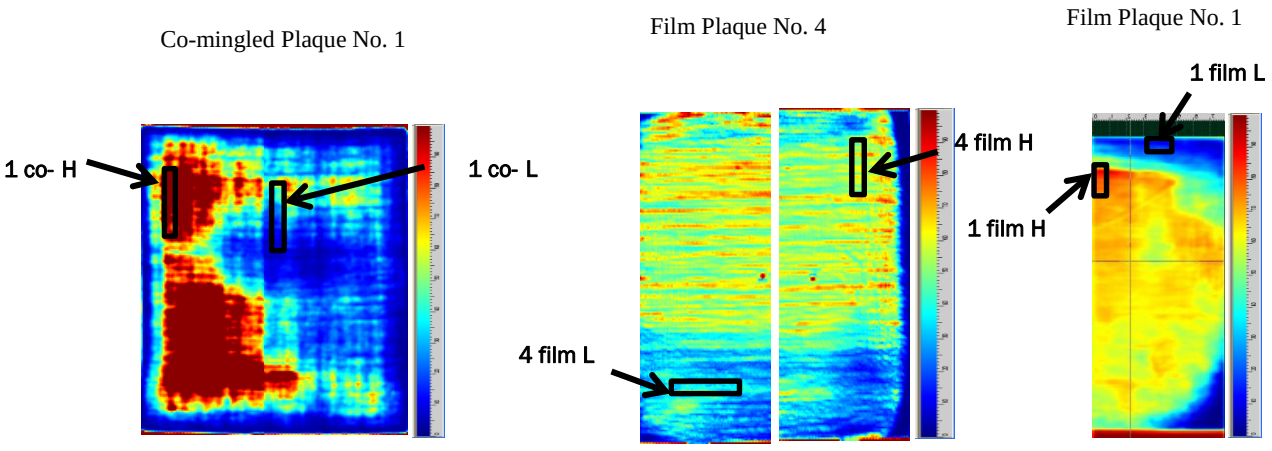

Figure 14. UT scans for CF/PEI plaques (a) co-mingled No. 1, (b) film No. 4, and (c) film No. 4.

Figure 14 shows the UT C-scans for film plaques (No. 1 and 4) and the co-mingled plaque No. 1. A sample was taken from the film plaque No.1 from the side which was dark blue (low transmission) and compared with a specimen from the center having a larger transmission. A similar procedure was applied to the specimens from the film plaque No. 4 and co-mingled plaque No. 1 [24]. The acid digestion on the CF/PEI film and co-mingled composites was performed using Methylene Chloride as per ASTM D 3171 [25]. Table 4 summarizes the results for the film and co-mingled plaques. The specimen which showed the high transmission had a fiber-volume fraction of approximately 49% with a void content of 0.78% compared to 53.46% fiber-volume fraction and 1.05% void content for the film 4 low-transmission sample. The film plaque No. 1 high-transmission specimen had a 53.05% fiber-volume fraction and 0.39% void content, while the low-transmission showed 55.71% fiber-volume fraction and 3.13% void content (this piece was taken from the edge, indicating high voids in that area). In contrast, the co-mingled plaque No. 1 showed lower fiber-volume fraction with 45.91% for high-transmission and 44.98% for low-transmission. For the voids, the results were approximately in the range between 2.41% and 2.79%, showing the higher voids than that of the film plaques. The acid-digestion tests were not conclusive in determining whether the porosity is localized to large voids or were the result of microporosity due to a lack of fiber wetting in the co-mingling specimens. The reduction in the UT frequency used (1 MHz for the co-mingled panels vs. 5 MHz for the film panels) was an indicator of inadequate wetting that is identified by the UT testing but not clear from the results of the acid digestion.

Table 4. Summary of acid-digestion test results CF/PEI physical properties for film and co-mingled composites.

Sample ID	Density (g/cc)	Weight % Fiber	Weight % Resin	Volume % Fiber	Volume % Resin	Void % Volume
4 Film H	1.51	57.454	42.546	48.55	50.67	0.78
4 Film L	1.53	62.355	37.645	53.46	45.49	1.05
1 Film H	1.54	61.625	38.375	53.05	46.56	0.39
1 Film H	1.52	65.607	34.393	55.71	41.16	3.13
1 co. H	1.48	55.595	44.405	45.91	51.68	2.41
1 co. L	1.47	54.83	45.17	44.98	52.23	2.79

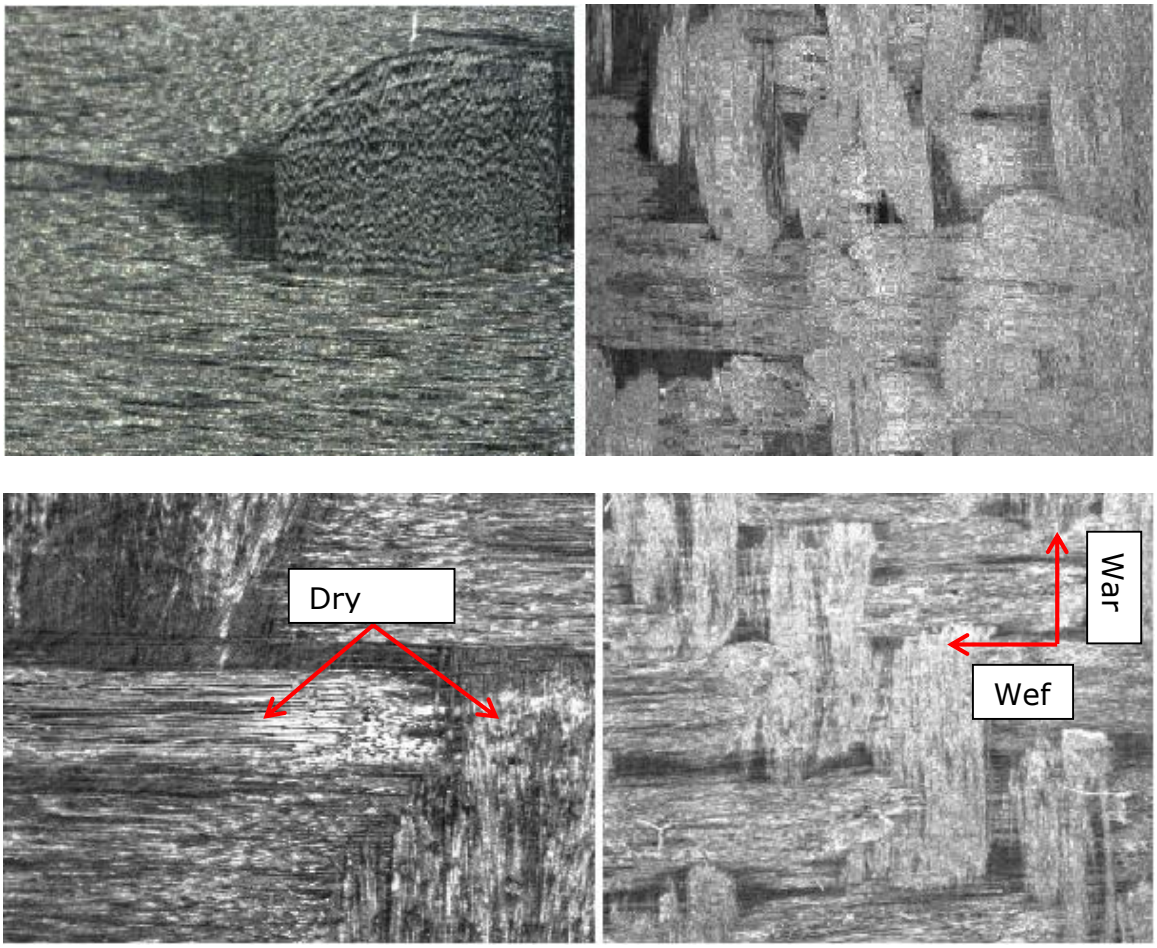

Figure 15. Optical microscope image of CF/PEI horizantal cross section (a) film specimen single bundle x5 (top left), (b) film specimen laminate in longitudinal and transverse direction x2 (top right), (c) co-mingled specimen single bundle x5 (bottom left), and (d) co-mingled laminate x2 weft and warp.

Optical microscopy was used to characterize the microstructure of CF/PEI film and co-mingled composites. Specimens were cut and polished horizontally and vertically to look at under the microscope. In Figure 15 (b), one laminate can be seen clearly at 2 times magnification in the film specimen showing a good fiber matrix wetting. When looking at 5 times magnification in Figure 15 (a), the fiber tow is in a round shape and the twill weave structure is in place with no resin-rich regions. On the other hand, in Figure 15 (d), the co-mingled laminate shows dry fibers running in both the longitudinal

and transverse directions. One observation was the dried fibers apparent in Figure 15 (c) which indicate poor wetting, unlike the film specimens (see discussion on this is in Chapter 5). The fiber tows in the co-mingled CF/PEI were flattened and spread out, which is opposite to the film specimens where a single filament is visible, which might indicate lower matrix content. Also, voids were found in some specimens entrapped between the warps and wefts (Figure 16), additional cross-sections are shown in Appendix C.

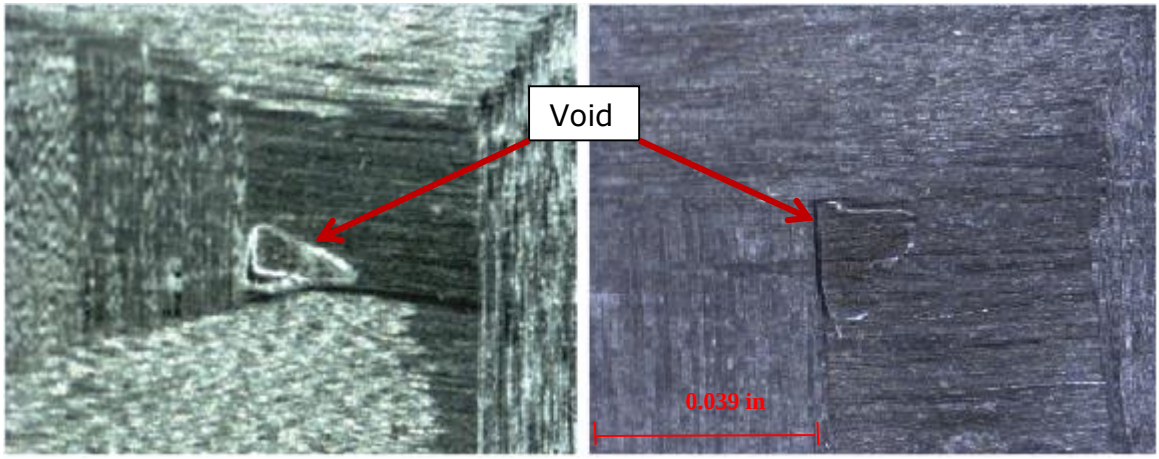

Figure 16. Air voids in film specimen, magnification x5.

5. Mechanical Characterization

In this chapter are described the mechanical tests that were performed on both film and co-mingled CF/PEI composite panels. The objective is to capture the effects on mechanical properties between the two techniques for making thermoplastics composites. Flexural, tensile, compression, and shear tests are performed. Carbon fiber J HTS40 (Tenax, Rockwood, TN, USA) is used to make the samples. The fiber is a high-strength PAN-precursor that is used for high-performance composites. The strength of the fiber for the 3K grade is 610 ksi with a modulus of 34.3 Msi with a filament diameter of approximately 7 micrometers [3].

The first test conducted was the flexural test and it showed inconsistent modulus results even within the same film plaque. Figure 17 shows the ultrasonic C-scan for plaque number 6. The scan shows the edges in blue due to low sound-wave transmission. The left side of the plaque shows a region with high through transmission. The variability in the flexural modulus is shown in Figure 17. Based on the initial UT scans it was decided to fabricate bigger panels in order to have homogenous testing specimens and three panels with the size of 20” by 16” were made. As per the ASTM D 7264, D 3039, D 2344, and SACMA SRM1R-94 mechanical test methods, each reported test value was based on an average of at least 5 samples.

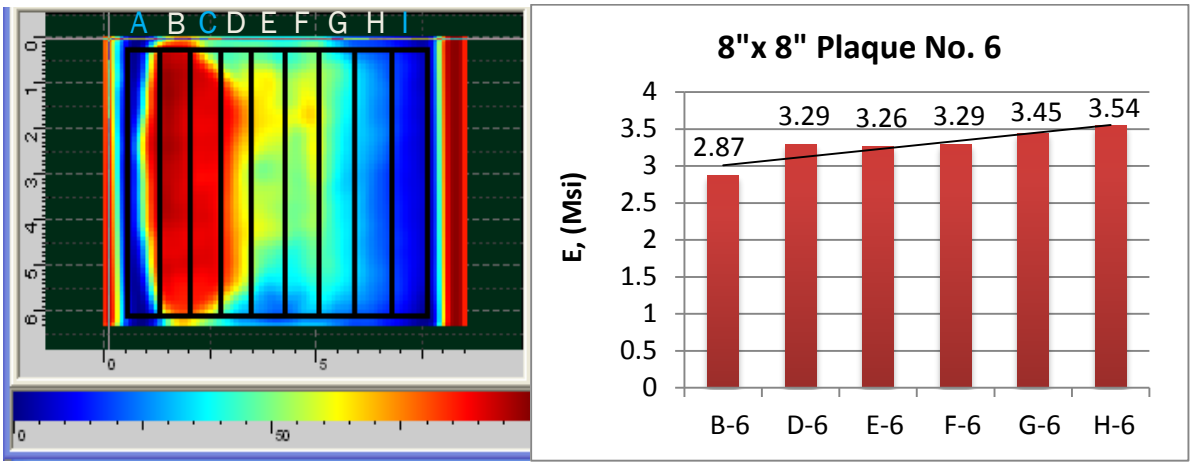

Figure 17. Plaque No. 6 UT and flexural modulus test showing the variation

5.1. Flexural Testing

Flexural tests were performed according to ASTM D 7264 "Flexural properties of Polymer Matrix Composite Materials", using procedure A with a three point loading method [26]. The first step was sample preparation where each panel was marked alphabetically using the panel number and the letters as the following example shows: CF and PEI Film Panel No. 1 so the samples were labeled as F1-A, F1-B, F1-C, F1-D, and F1-E. A bench-top saw was used to cut the sample to the specified width. The saw was cooled using water to minimize the damage to the edges of the specimens. The flexural-test sample geometry was based on the composite thickness which in this case was 0.125", the width was 0.51" and a length of 6" to get a test span length of 1:32 ratio (around 4 inches for the test span). Five samples were extracted from the three panels in the CF/PEI film category: F1, F2, and F3 and for co-mingled panels: Co.1, Co.2, and

Co.3 with (A, B, C, D, and E for each sample) for a total of 40 samples. An electromechanical material test system shown in Figure 18 (314R; Test Resources, Shakopee, MN, USA) was used for the flexural testing using the ASTM-recommend speed of 0.04 in./min [26].

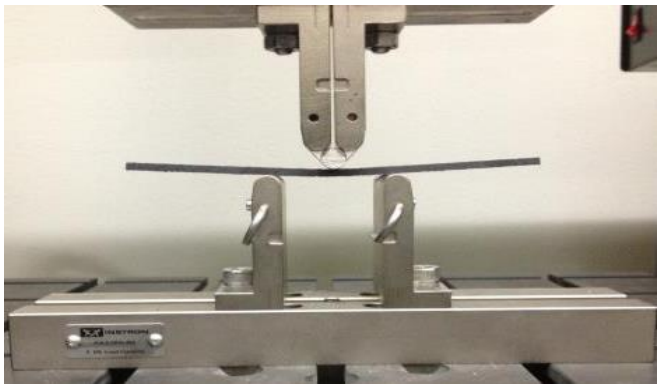

Figure 18. Flexural test setup for a CF/PEI specimen under three point loading

The CF/PEI film samples' resistance for bending was higher than the co-mingled and the failure mode was brittle. The flexural stress of the first film plaque was 135.287 ksi and the flexural strain was 0.0161 in/in, where for plaque No. 2 stress is 102.9 ksi and strain of 0.0160 in/in, and the plaque No.3 had a stress of 105.98 ksi and strain of 0.0139 in/in. The modulus of the film samples were 9.147, 8.220, and 8.334 Msi for F1, F2, and F3, respectively. For co-mingled CF/PEI samples Co-1 flexural stresses were 60.053, Co-2 58.868 and Co-3 53.449 ksi. The strains were 0.0167, 0.0140, and 0.0143, respectively. The co-mingled samples were showing a higher deflection than the film samples. The composite specimens start to fail early and the damage continues to propagate after the

first failure. It was decided to take the strain at the ultimate flexural stress because the sample strength drops slowly without a sharp failure as shown in Figure 19.

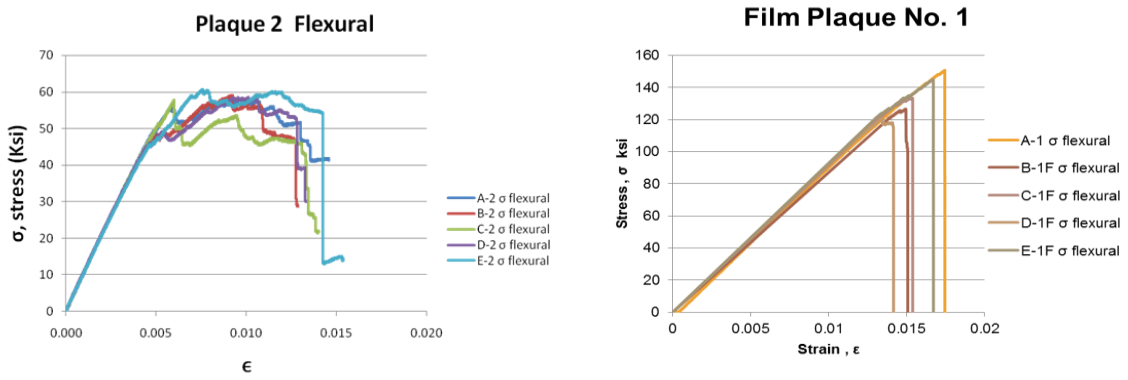

Figure 19. Stress strain flexural curves: a) co-mingled plaque Co-2 (left) b) film plaque F-1 (right).

An optical microscope was used to observe the specimens during testing. The damage initiation was observed in the co-mingled specimen at the top region under compression. This crack continued to grow through the thickness causing the failure eventually. In the film specimen, the failure was brittle and it was not easy to capture the damage progression because of the brittle failure mode. Table 5 summarizes the flexural properties for both the film and co-mingled composites. The test data for all the flexural tests can be found in Appendix B.

Table 5 Summary for CF/PEI flexural results for both film and comingled samples

Plaque No.	E (Msi)	Std (Msi)	σ_u (Ksi)	Std (ksi)	ϵ_u	std
F-1	9.147	0.258	135.287	12.583	0.0161	0.0012
F-2	8.223	0.531	102.902	7.644	0.0160	0.0010
F-3	8.334	0.521	105.977	11.470	0.0139	0.0009
Co-1	8.452	0.292	60.053	5.043	0.0089	0.0014
Co-2	10.218	0.116	54.516	5.286	0.0062	0.0010
Co-3	9.652	0.196	49.072	2.992	0.0061	0.0006

5.2. Tensile Testing

5.2.1. Tabbing

A test is counted successful if the failure occurs in the central gauge area of the specimen. However, significant challenges occur in testing FRP composites in order to obtain successful tests due to stress concentrations in the grip region. As the axial load requires higher grips forces to carry the test at higher loads, this might further crush the samples' surface, resulting in grip failure. Adding tabbing material onto the specimen faces can prevent surface damage from higher grip forces. The second advantage is that tabbing will increase the cross-sectional area and this makes the gauge section more likely to be the location of failure. There are three factors in tabbing that will affect its performance and these are: tab material, adhesive selection, and tab geometry design.

In this study, layers of G10 standard glass fiber and epoxy composite of 0.125-inch thickness are used on each side (tabbing was performed at Interteck lab, Pittsfield, MA, USA). Secondly, adhesive selection is an important element in tabbing because it is affected by the surrounding temperature and the thickness of the layer that needs to result in an efficient load transmission. The adhesive material also needs to be compatible with both materials. In this study, the Hysol 120 HP adhesive is selected for the tabbing material. The last part of the tabbing design is to choose a tapered or un-tapered tabbing geometry. The impetus for a tapered design is to have a minimal stress concentration near the end of the tab because there would otherwise be a sudden change in cross-section. Figure 20 shows a finite-element analysis mesh of tab configurations reported in "Tabbing Guide for Composite Test Specimens" performed by the Office of Aviation Research [27]. The typical tapered angle is approximately 7º. On the other hand, in the un-tapered tab more stresses are generated near the surface when compared with the tapered tab design [28]. In unidirectional- or multidirectional-composites tension specimens, a taper of approximately 7–10º is recommended as per ASTM 3039 to have the proper failure within the gauge area. For compression testing, an un-tapered tab is preferred because the specimen will be end-loaded as per the Suppliers of Advanced Composite Materials Association (SACMA) SRM 1R-94 test method [29].

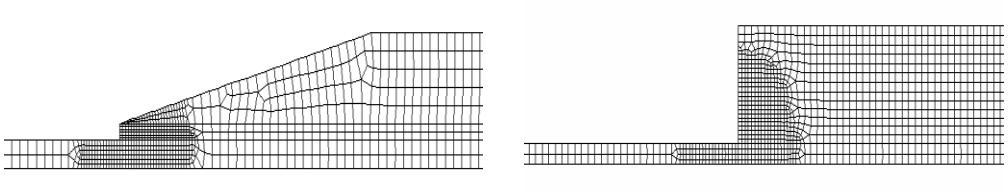

Figure 20. Finite-element mesh in the tab-termination region: a) tapered tab (left) b) un-tapered tab (right) [27].

5.2.2. Open Hole Tension (OHT)

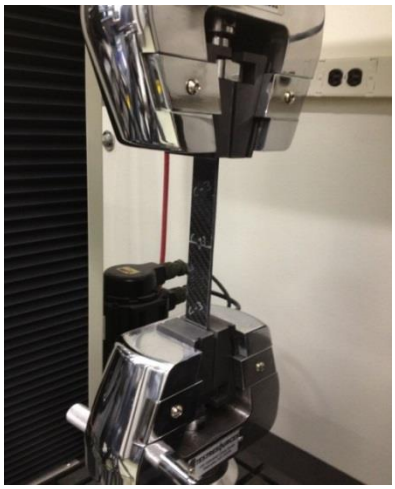

Figure 21. Test setup for CF/PEI sample.

ASTM D 5766 “Standard Test Method for Open-Hole Tensile (OHT) Strength of Polymer Matrix Composite Laminates” was used for open hole testing of the CF/PEI composites [30]. Having a controlled failure in the middle of the specimen with a stress concentration area (i.e. the hole) resulted in an acceptable failure without using tabbing. Also, OHT results are usually used in the aerospace industry to give ultimate material

strengths considering composite parts having fasteners or bolts [30]. The OHT samples had the same dimensions as the unnotched samples in ASTM D 3039 which will be described later in this report. The important consideration is to have a ratio of 6 for the sample width to the hole diameter (W/d). The hole is centered in a 10" long and 1" wide specimen [30]. A 0.167" diameter hole was drilled carefully in order to avoid delamination of the plies by using a backing wooden plate.

The 314R electromechanical universal testing machine was used with mechanical grip control (Figure 21). Closing the grips was challenging because a high torque is needed to tighten onto the samples in order to avoid slipping at high stresses while at the same time over tightening can result in a failure at the grips. In our case, it was found that around 25 lb-ft of tension force developing during gripping was needed to close both grips and conduct the test without slipping or grips failure. Then, tests were carried using a displacement-controlled mode with 0.04 in/min as per the ASTM D5766 standard. A representative set of stress-strain curves are shown in Figure 22. The average results for the three films were obtained as follows: 52.13, 54.11, and 50.77 ksi for plaques F-1, F-2, and F-3, respectively. All of the samples failed at the hole and there was good repeatability with standard deviations of 1.87, 3.25, and 3.78 ksi, respectively. Similarly, co-mingled specimens were tested and the results for Co-1, Co-2, and Co-3 came up to be 49.2 ksi, 55.7 ksi, and 55.0 ksi.

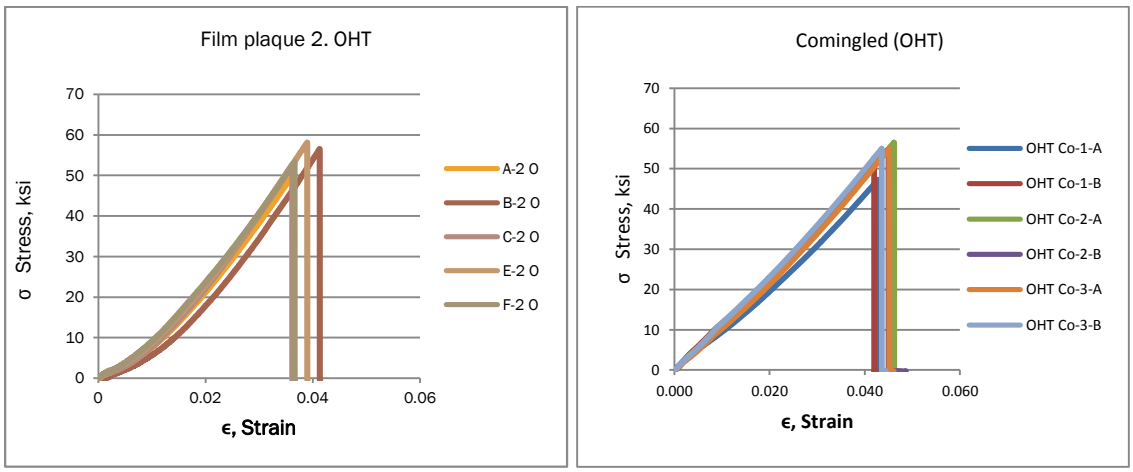

Figure 22. OHT stress vs. strain curves: a) film specimens (left), b) co-mingled specimens (right).

5.2.3. Unnotched Tension Testing

The unnotched CF/PEI specimens were 10" long and 1" wide. The specimens were tested at a speed of a 0.04 in/min for both the film and co-mingled composites. Figure 23 shows the teeth-grip indentations on the surface. Also, an extensometer was used to measure the tensile modulus for the linear region and removed before failure. First, film samples were tested up to fracture. The specimens showed a brittle failure with the following average tensile strength (5 specimens per plaque): 104.93, 128.77, and 119 ksi for plaques F-2, F-4, and F-5, consecutively. Also, initial fabric failure was noticed and recorded as follows: 94.31, 119, and 114.9 ksi for the film samples and was near the ultimate stress as in table 6. For the co-mingled specimens, damage initiation (determined from load-displacement records) started earlier in the loading cycles and

were recorded as (average of 5 specimens per plaque): 67.87, 77.83, and 79.86 ksi. The failure stresses for F-2, F-4, and F-5 were 89.34, 99.53, and 106.64 ksi respectively (Table 6). Another observation in the co-mingled specimens, when samples were broken, was that dry fibers snapped leaving a fiber particulate cloud after failure unlike film samples where the fracture was clean and neat. For the modulus, the results were comparable. For the co-mingled samples, the modulus recorded was: 8.15, 8.94, and 8.73 Msi. On the other hand, the average modulus values in the film samples were 8.99, 9.43, and 9.36 Msi (table 6). The modulus was measured between the strain values of 0.3 and 0.5%. Table 6 shows a comparison of the stress concentration factors in the film and co-mingled specimens. The co-mingled specimens show a higher stress concentration factor compared to the film specimens especially when considering the damage-initiation criteria.

Figure 23. CF/PEI tabbed tensile sample with tapered ends.

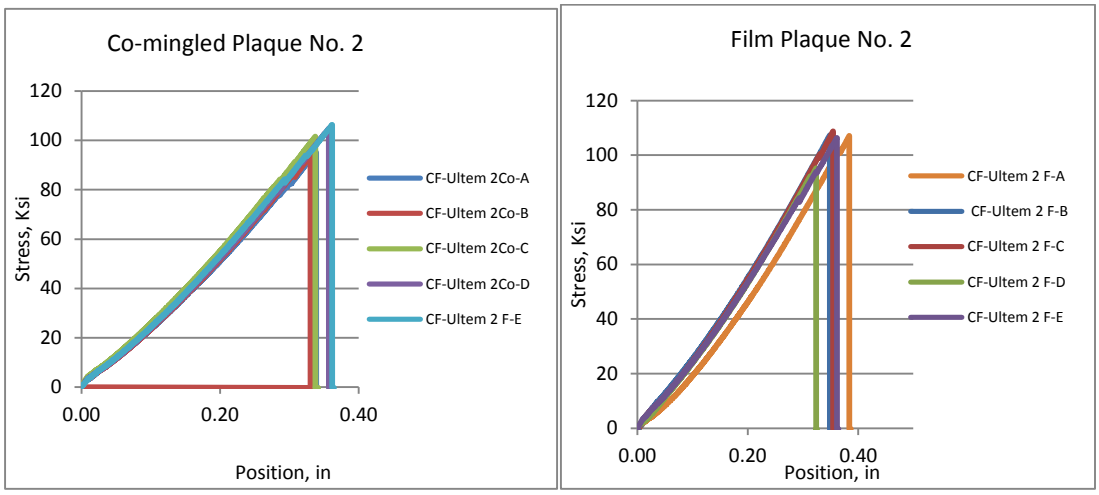

Figure 24. tensile stress vs. position curves for: a) co-mingled specimens (left), (b) film specimens (right).

Table 6 Summary for CF/PEI Ultimate tensile and damage initiation strengths for CF/PEI for both film and comingled composites.

Plaque No.	E (Msi)	Std (Msi)	σin (Ksi)	Std (ksi)	σ f (Ksi)	Std (ksi)
F-2	8.990	0.32	94.310	10.30	104.930	5.50
F-4	9.430	0.93	119.000	18.48	128.770	9.79
F-5	9.360	0.62	114.900	16.31	119.000	14.63
Co-1	8.150	0.45	67.870	5.49	89.340	5.57
Co-2	8.940	0.26	77.830	4.89	99.530	5.14
Co-3	8.730	0.10	79.860	6.15	106.640	8.09

Table 7 Stress concentration factors in film and comingled specimens

Specimen Type	Avg. Ultimate Stress (Msi)	Std	Avg. Initiation Stress (Msi)	Std
UNT Film	0.1184	0.0177	0.1098	0.0149
UNT Comingled	0.0985	0.00745	0.0752	0.00943
OHT Film	0.0529	0.00370	0.0529	0.00370
OHT Comingled	0.0533	0.00344	0.0533	0.00344
Stress Concentration Factor				
Film	2.24		2.08	
Comingled	1.85		1.41	

5.3. Compression Testing

Several testing approaches have been proposed for compression testing of fibrous composite materials. These include the ASTM D 3410 Celanese compression test method, a flexural sandwich-beam method [31] in the combined loading compression (CLC) test method. ASTM D 3410 Celanese compression test method was developed by Celanese Corp in 1970's but it has been found to be sensitive to sample preparation and the complexity of the fixture. Another method using a flexural test compression region of a sandwich sample was proposed in 1993 and became a standalone test in the ASTM D 5467 for composites [31]. The procedure still required significant sample preparation and ensuring the adhesion of the factsheets through the complete test. In early 1980's the Boeing Company, in collaboration with Hercules Inc. modified a compression test method derived from ASTM D 695 that was used for unreinforced plastics [31]. The

main change was in the sample shape which moved from the typical dog-bone to the straight-and-tabbed specimen geometry. This test method was later adopted by the Suppliers of Advanced Composite Materials Association (SACMA) SRM 1R-94 [29]. It became popular because the simple fixture design and weight made it easy to deal with. Further, the specimen shape meant that a smaller amount of material was required. To overcome the issues with specimen buckling, the gauge length was reduced which resulted in making it difficult to use strain measurements unless an un-tabbed sample is used. This method used an end load to apply the force that can be problematic in some instances if end crushing occurs, preventing failure from occurring in the critical gauge section of the coupon.

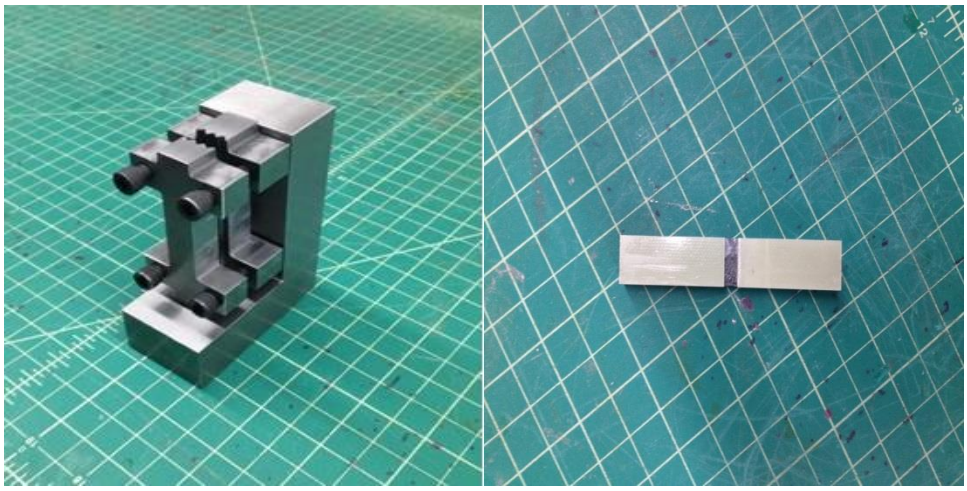

Figure 25. (a) Modified ASTM D 695 compression test-method fixture for CFRT (left), (b) tabbed compression CF/PEI specimen (right).

The ASTM D 695 test method was selected because of its simplicity and the small size of the testing specimens. Using SACMA drawings [29], the fixtures were fabricated at the University of Wisconsin-Milwaukee machine shop for both the strength and modulus measurement configurations. The fixture was manufactured with fine threads allowing precise torque application on the specimen. The specimen dimensions were 3.18'' in length, 0.5" in width, and 0.120" thickness. The specimens were tabbed as shown in Figure 27. the specimens were tested in displacement-controlled mode at a rate of 0.05 in/min to apply end loads on the sample [29]. The average results were as follows: film F-3 was 104.35 ksi; F-4 A and B were 119.28 and 95.16 ksi, respectively, and F-5 was 99.17 ksi. For co-mingled plaques no. 1 and 3 (5 specimens per plaque), the stresses were 50.16 and 46.98 ksi, showing a significant reduction compared to the CF/PEI film samples as shown in table 8. The failures occurred in the gauge portion and most of the failures were clean and normal to the force axis. A few samples failed at a 45^{o} angle. The compression test was very successful with failures occurring in the gauge portion. Most of the failures were clean and normal to the force axis. A few samples failed at 45^{o} angle as shown in Figure 29.

Table 8 Summary of CF/PEI Compression strength results of comingled and film plaques

Plaque No.	σ (Ksi)	Std (ksi)
F-3	104.35	2.22
F-4	119.28	11.1
F-4	95.16	5.12
F-5	99.17	4.28
Co-1	50.16	2.92
Co-3	46.98	7.75

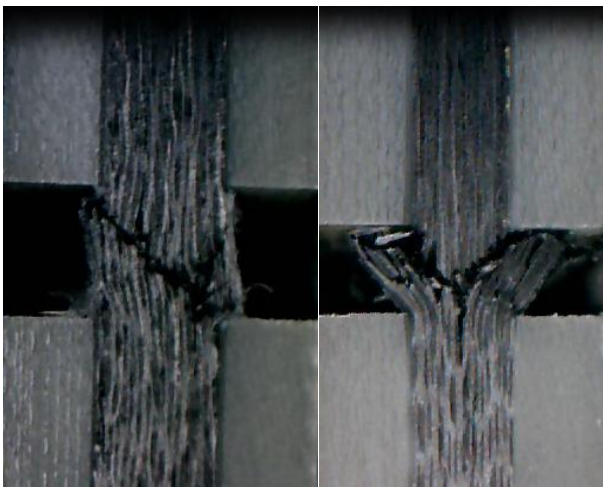

Figure 26. Compression specimens' failure mode (a) co-mingled CF/PEI failing at 45 (left), (b) film CF/PEI.

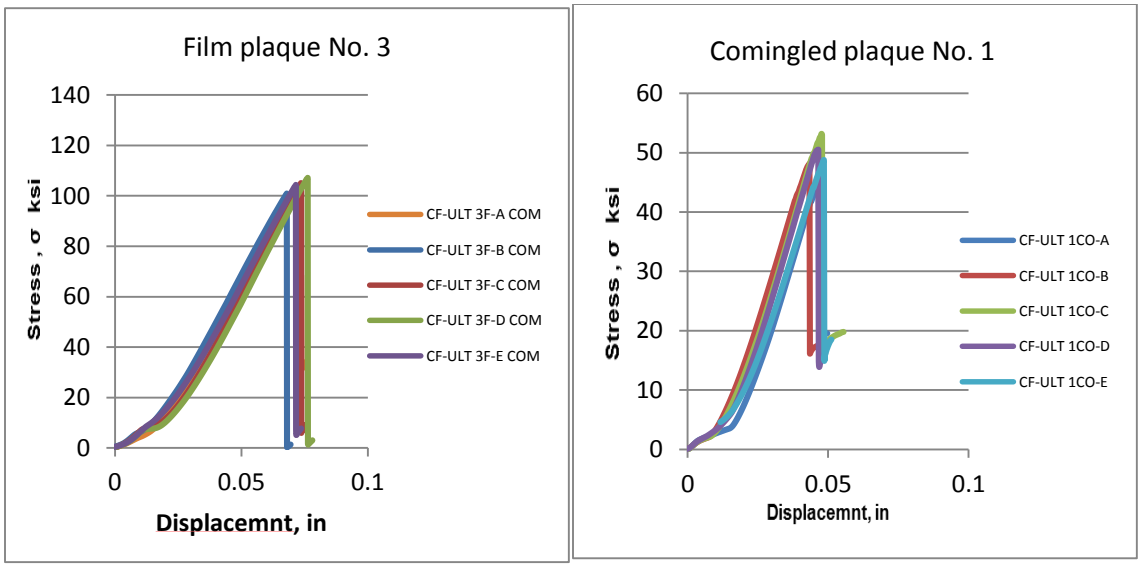

Figure 27. Compression stress vs. position curves for: a) co-mingled specimens (left), (b) film specimens (right).

5.4. Short Beam Shear (SBS)

Short-beam shear (SBS) tests were conducted using the ASTM D 2344 “Standard Test Method for Short-Beam Strength of Polymer Matrix Composite Materials and Their Laminates” [32]. The specimen resembles a three-point bending setup but with a short support span. SBS is used to determine an approximate value for the interlaminar shear strength of fiber-reinforced plastics (Figure 31). The specimen dimensions are a function of plaque thickness. The length was 6 times the thickness and the width was twice the thickness. In this case the plaque thickness was 0.12” giving sample dimensions as follows: 0.7” in length and 0.23” in width. The samples were selected from different areas using the UT results as a guide. The test speed used was 0.04 in/min and the nose was lowered until it touched the samples in order to push it against the two supports with a span of 0.47”. The specimen was oriented transverse to the force direction and the load increased until the sample fractured. Film samples had a brittle failure and the load–displacement curves were linear, unlike co-mingled samples where the failure was gradual and the fibers broke slowly (Figure 31). The maximum shear stresses obtained in the film plaques using the SBS test were 9.01, 8.52, and 9.75 ksi for film plaques 1, 2, and 3, respectively. These were based on averaging the results from 5 specimens from each plaque. On the other hand, co-mingled results had high variability as plaque 2 had a value of 6.3 ksi, plaque 3 had a value of 8.39 ksi, and plaque 1 was found to be 11.85 ksi (table 9).

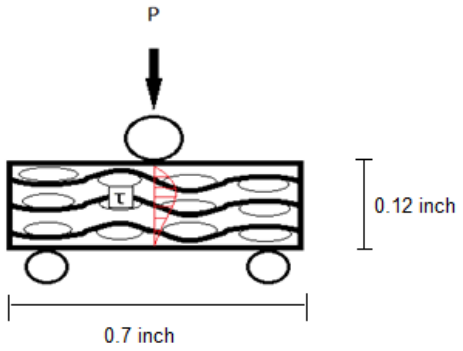

Figure 28. SBS sketch for the test setup and force application.

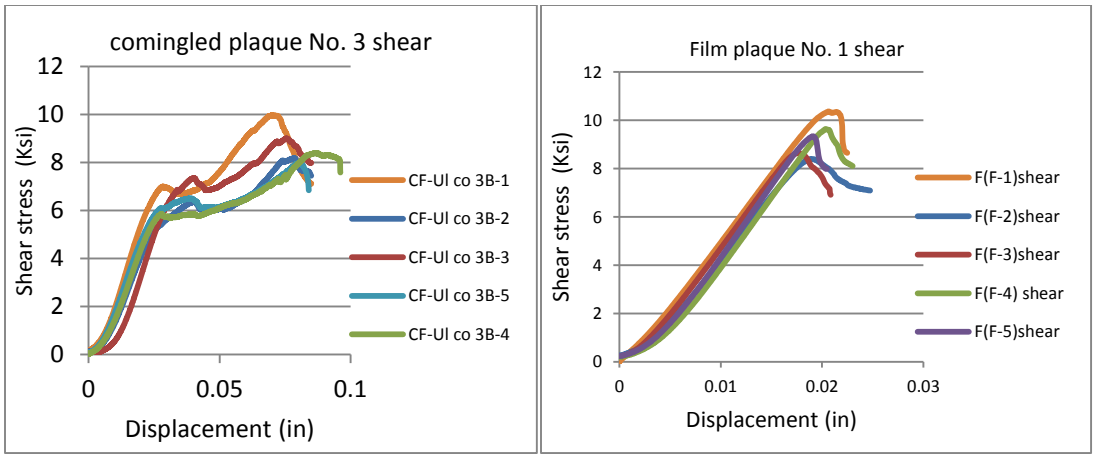

Figure 29. SBS stress vs. displacement for: a) co-mingled specimens (left), (b) film specimens (right).

Table 9 summary of Short Beam Shear (SBS) failure strength of CF/PEI composites

Plaque No.	σ_{SBS} (Ksi)	Std (ksi)
F-1	9.007	0.58
F-2	8.515	0.2003
F-3	9.749	0.286
Co-1	11.850	2.13
Co-2	8.386	0.45
Co-3	6.301	0.34

5.5. Dynamic Mechanical Analysis (DMA)

Dynamic–mechanical analysis (DMA) is a technique that measures the dynamic stiffness in a material due to dynamic stress or strain stimuli. The response to the stimuli is divided into an elastic response and a viscous response. Elastic response accounts for the elastic energy stored in the material. Viscous response results from the phase lag angle (δ) between a sinusoidal applied stress (e.g. $\sigma = \sigma_o \sin \omega t$) and a measured strain (or vice versa) due to the viscoelastic behavior of most materials. The elastic response is measured by the elastic modulus; the viscous response is measured by the loss modulus. Damping ($\tan \delta$) is the tangent of the phase angle; it is the ratio of the loss to storage modulus. For a rectangular specimen and a single cantilever clamp, movement is restrained in all directions at one end and only vertical displacement is allowed at the other end [33]. The study was carried out on a DMA system (Q800; TA instruments, New Castle, Delaware) using single-cantilever mode (Figure 34). A controlled displacement of 15 μm was used. The test specimens were approximately (0.7 x 0.45 x 0.124 in) in length, width, and thickness, respectively. The test parameters were chosen to comply with the general recommendations of the ASTM D4065-12 [34] standard. The two different sets of composite specimens (co-mingled and film specimens) were tested at a constant frequency of 1.0 Hz. During the loading, a temperature range of 68–572 ˚F was applied at a rate of 9 ˚F/min. The storage-modulus results show a clear difference in modulus between the co-mingled and film specimens. The higher glass transition temperature is seen in the co-mingled specimens but this may be due to voids in the

composite. The first and second heating curves in the film specimens yield similar results.

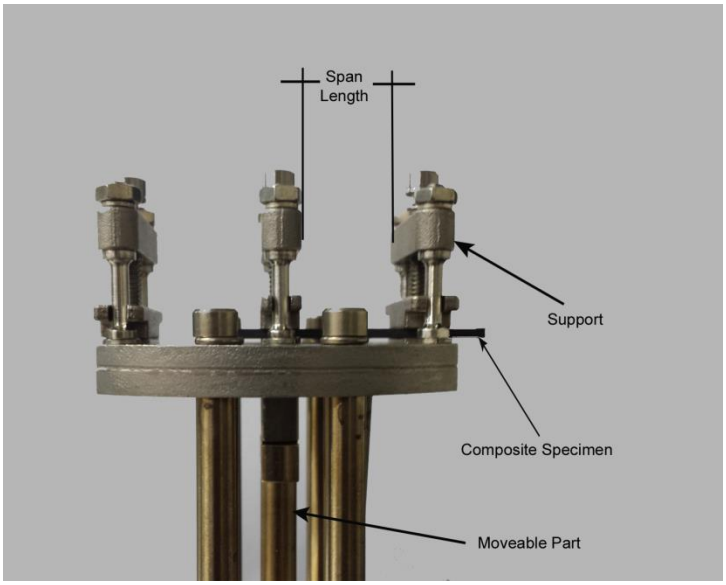

Figure 30. Single-cantilever DMA test setup.

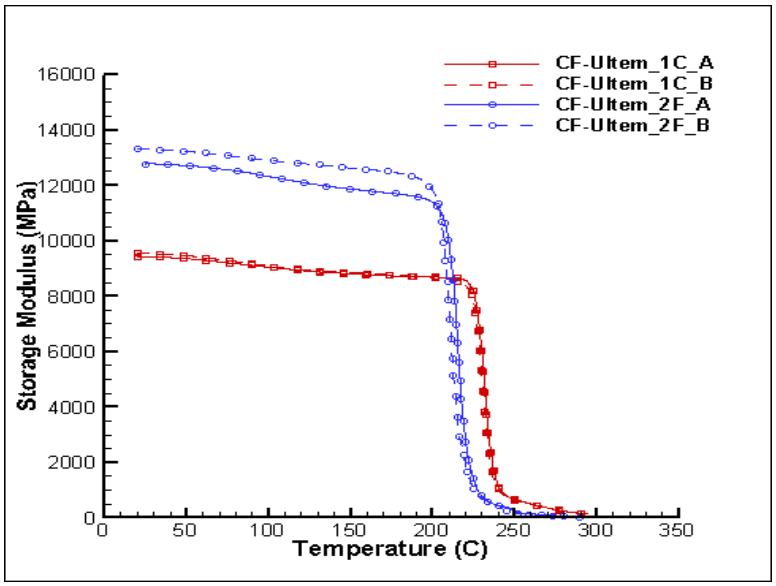

Figure 31. Storage modulus vs. temperature for CF/PEI, both film and co-mingled specimens.

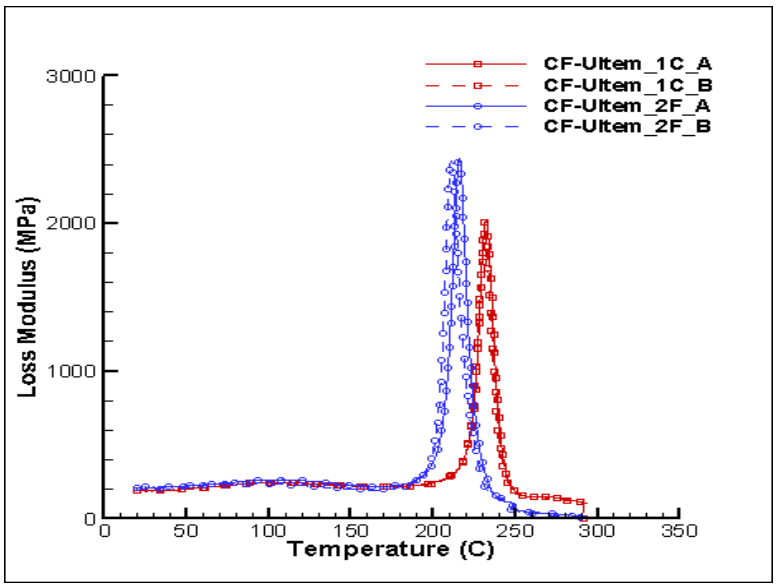

Figure 32. Loss-modulus plot vs. temperature for CF/PEI film (blue) and co-mingled specimens (red).

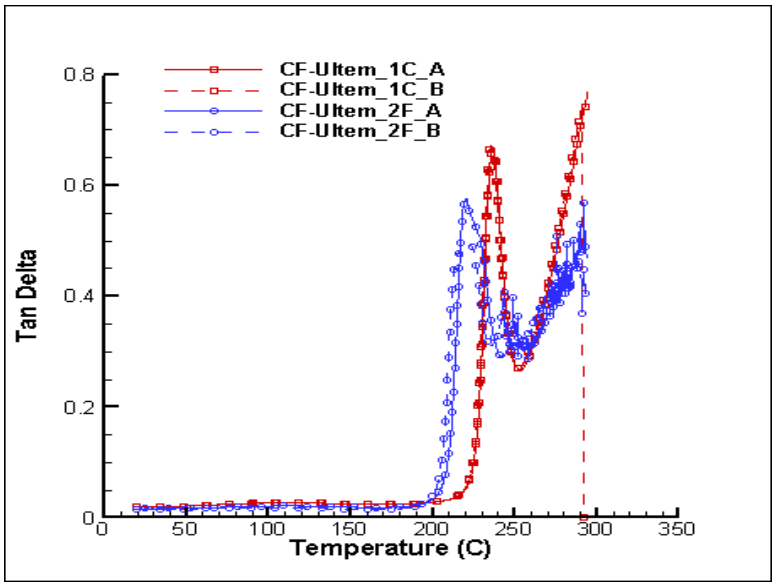

Figure 33. Tan delta plots for CF/PEI specimens, film (blue), co-mingled (red).

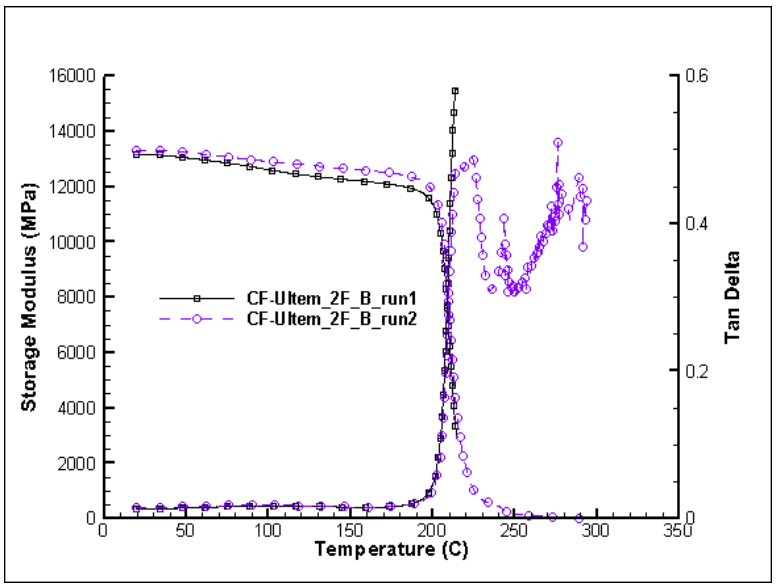

Figure 34. First and second heating curves for storage modulus and tan delta for CF/PEI film specimens (Plaque F-2).

6. Results and Discussion

The co-mingling technique has saved approximately 35.71% of processing time, 100 ˚F lower temperature and 56.25% of the pressure used compared to the film laminates. However, further optimization may need to be performed to further improve the mechanical properties, as these plaques were not completely cured and there is no guideline for fabricating co-mingled thermoplastics because it depends on individual plastics characteristics. Below is a summary of the main observations from the testing performed on the two material systems:

- The acid digestion tests correlated with the porosity estimates in the film specimens from the UT C-scans but did not correlate directly with the porosity in the co-mingled specimens. This may be due to the waviness present in the co-mingled specimens or the lack of adequate wetting of the fibers in specimens. Note that the transducer frequency had to be changed from 5 MHz in the film plaques to 1 MHz in the co-mingled plaques. This indicates greater attenuation in the co-mingled plaques. The UT method is thus recommended for evaluating CFRT panel quality.
- The microstructure between the co-mingled and the film specimens shows dry areas in different regions, insufficient consolidation, and lack of fibers wetting. However, the film samples showed better wetting although there were high-resin regions. Voids were observed in areas such as the cross between warps and wefts which maybe a further area of research to find methods to reduce this.

- In the flexural tests, the co-mingled specimens showed a reduction of 49.9% in strength, 53.9% in strain, and a slight increase in modulus with around 10% compared to film. On the top of the flexural specimen a compressive stress is generated and on the bottom the specimen is in tension. The optical microscope used to record the specimen showed the failure in the co-mingled specimen to initiate in the top face (compression) and went through the thickness until it reached the bottom face. This correlates with the compression results that was lower by 53.51% compared to the film specimens. This suggests that bending properties in flexure are limited by the compression strength of the material and not by the tension strength.
- The flexural test which was used to select the optimum temperature was not showing real modulus results because it is a function of geometry (thickness) and not real temperature dependence only. Therefore, extra porosity may result in increased modulus at the expense of other mechanical properties.
- The notched tensile results show that the strength of both film and co-mingled specimens are reduced by half for ultimate stress as a result of the hole. For damage initiation stress, co-mingled specimen strength was reduced by approximately 70% compared to film that showed a reduction of around 50%.
- The unnotched tensile strength, for co-mingled specimens was 16.21% lower in ultimate-tensile stress and 7.05% lower in modulus than film. This is because usually tensile strength is fiber-property dominated, although there are other aspects that affect axial load such as void content and fiber waviness along the plaque. The

tension tests are not recommended for development of curing recipes for CFRT composites.

- The compression specimens show that co-mingled had lower failure stresses than the film by 53.51%. The strength is almost similar to the flexural strength which indicates that the region in compression failed first.
- The proposed compression fixture from (SACMA) SRM 1R-94 or modified ASTM D695 is suitable for compression testing of CFRT composites. This could be a good, quick test to verify the consolidation quality.
- From the storage-modulus plot (Figure 35), the film specimens are, on average, 35% stiffer than the co-mingled composite specimens at room temperature.
- From the *tan δ* plots (Figure 37), the glass transition temperature (T_g) for both sets of specimens could be determined from the peaks of the *tan δ* curves. The glass transition temperature for the co-mingled specimens is around 245 ºC while that for the film samples is around 225 ºC. The co-mingled composites thus have a higher T_g and this is also confirmed by the loss-modulus plots (Figure 36) and from the degradation pattern seen for the storage modulus at the higher temperatures (Figure 36). The *tan δ* plots also show a higher damping level for the co-mingled specimens (around 20% higher) as characterized by higher *tan δ* peaks for the co-mingled specimens. These results correlate with the other observations which indicate higher porosity levels in the co-mingled specimens.
- The first and second heating curves for a film specimen (Figure 38) show almost matching behavior for the storage modulus and *tan δ* plots. The degradation pattern in

the storage modulus and the *tan δ* peaks match for both runs. The second heating shows a slightly stiffer behavior of the composite for the second run before the glass transition temperature.

7. Conclusion

In conclusion, a total of 134 specimens were tested to investigate the performance of film and co-mingled carbon-fiber reinforced thermoplastic (CFRT) composites. In this study, a polyetherimide (PEI) fiber was co-mingled with carbon-reinforcing fiber and then woven into fabrics and processed using compression-molding techniques. Co-mingling thermoplastic fibers is a promising technique that shortens the process cycle time. Pre-laminated specimens were also fabricated using films of PEI layered between layers of a twill carbon-fiber materials. The panel quality was assessed using the immersion UT technique. After that, samples were prepared for mechanical characterizations under different loading mechanisms: in tension, flexure, compression, and shear. These tests were used to understand the mechanical performance, the strengths, and drawbacks of each technique and how it was related to processing conditions. This thesis has identified the benefits and limitations of the testing methods that can be used in development of new CFRT composite systems. Further work is needed in order to optimize processing parameters of the co-mingled method and to understand the important factors that limit its use. Energy absorption characteristics need to be compared between two systems as thermoplastics have superior impact properties. Additional research on the UT parameters used in CFRT and how they relate to internal microstructure needs to be investigated. Co-mingling quality, fiber diameter size, and wrinkles that might be generated during processing are some of the areas that need further research in order to help making CFRT composites. Specifically, more research

on assessing the quality and variability of the co-mingling of the PEI/CF needs to be performed.

8. References.

1. Chung, D.D.L., *Carbon Fiber Composites*1994: Butterworth-Heinemann. 7.

2. Delhaes, P., *Fibers and composites*. Vol. 2. 2003, New York, USA: CRC Press.

3. Tenax, T., *HTS40, Toho Tenax®- J*, 2012.

4. Raghavendra R. Hegde, M.G.K., Atul Dahiya. *Polymer Crystallinity*. 2014 [cited 2014 22 April 2014]; Available from:http://www.engr.utk.edu/mse/pages/Textiles/Polymer%20Crystallinity.htm.

5. *ULTEM™ Film Resin data sheet*. 2014 [cited 2014 10 March 2014]; Available from: http://www.sabic-ip.com/gep/Plastics/en/ProductsAndServices/ProductLine/ultem.html.

6. Bernet, N., et al., *Commingled yarn composites for rapid processing of complex shapes.* Composites Part A: Applied Science and Manufacturing, 2001. **32**(11): p. 1613-1626.

7. Svensson, N., R. Shishoo, and M. Gilchrist, *Manufacturing of thermoplastic composites from commingled yarns-A review.* Journal of Thermoplastic Composite Materials, 1998. **11**(1): p. 22-56.

8. Choi, N., H. Yamaguchi, and K. Takahashi, *Fracture behavior of unidirectional commingled-yarn-based carbon fiber/polyamide 6 composite under three-point bending.* Journal of composite materials, 1996. **30**(7): p. 760-784.

9. Ye, L., V. Klinkmuller, and K. Friedrich, *Impregnation and consolidation in composites made of GF/PP powder impregnated bundles.* Journal of Thermoplastic Composite Materials, 1992. **5**(1): p. 32-48.

10. Klinkmuller, V., et al. *Impregnation and consolidation of different GF/PP commingled yarns*. in *Proceedings Tenth International Conference on Composite Materials. Whistler, BC, Canada*. 1995.

11. Braches, E. *Proceeding of Techtextil Symposium*. in *Techtextil Symposium*. 1991. Frankfurt, Germany.

12. Ye, L., et al., *Consolidation of unidirectional CF/PEEK composites from commingled yarn prepreg.* Composites science and technology, 1995. **54**(4): p. 349-358.

13. Santulli, C., et al., *Void content measurements in commingled E-glass/polypropylene composites using image analysis from optical micrographs.* Science and Engineering of Composite Materials, 2002. **10**(2): p. 77-90.

14. Ye, L., A. Beehag, and K. Friedrich, *Mesostructural aspects of interlaminar fracture in thermoplastic composites: Is crystallinity a key?* Composites Science and Technology, 1995. **53**(2): p. 167-173.

15. Ye, L. and K. Friedrich, *Mode I interlaminar fracture of co-mingled yarn based glass/polypropylene composites.* Composites Science and Technology, 1993. **46**(2): p. 187-198.

16. Ye, L. and K. Friedrich, *Interlaminar fracture of commingled-fabric-based GF/PET composites.* Composites, 1993. **24**(7): p. 557-564.

17. Gardiner, G. *Thermoformable Thermoplastics Composites*. compositesworld, 2010. **2013**.

18. Leeser, D. and B. Banister. *Amorphous thermoplastic matrix composites for new applications*. in *International SAMPE Technical Conference, 21 st, Atlantic City, NJ, Proceedings*. 1989.

19. Béland, S., *High performance thermoplastic resins and their composites*1990, New Jersey, USA: William Andrew.

20. Kapadia, A., *Non Destructive Testing of Composite Materials*. TWI Ltd, 2006.

21. *TecView Ultrasound Test Inspection and Analysis user's Guid, v 1.43*, 2008.

22. Yang, P. and R. El-Hajjar, *Porosity Defect Morphology Effects in Carbon Fiber–Epoxy Composites.* Polymer-Plastics Technology and Engineering, 2012. **51**(11): p. 1141-1148.

23. Long, A., C. Wilks, and C. Rudd, *Experimental characterisation of the consolidation of a commingled glass/polypropylene composite.* Composites science and technology, 2001. **61**(11): p. 1591-1603.

24. *Constituant Content of Composite Materials*, 2014, Interteck

25. ASTM, *ASTM D 3171, "Constituent Content of Composite Materials,"*2009.

26. ASTM, *ASTM D 7264, "Flexural Properties of Polymer Matrix Composite Materials,"* 2007.

27. Adams, D.O.A.a.D.F., *TABBING GUIDE FOR COMPOSITE TEST SPECIMENS*, 2002, U.S. Department of Transportation.

28. ASTM, *ASTM D 3039, "Tensile Properties of Polymer Matrix Composite Materials,"*2008.

29. Association, S.o.A.C.M., *Compressive Properties of Oriented Fiber-resin Composites*, 1994.

30. ASTM, *ASTM D 5766, "Tensile Strength (Open Hole) of Polymer Matrix Composite Laminates Testing,"*2011.

31. Adams, D.D. *Current compression test methods*. composites world, 2005.

32. ASTM, *ASTM D 2344, "Standard Test Method for Short-Beam Strength of Polymer Matrix Composite Materials and Their Laminates,"*2000.

33. Menard, K.P., *Dynamic mechanical analysis: a practical introduction*2008: CRC press.

34. ASTM, *ASTM D 4065, "Standard Practice for Plastic: Dynamic Mechanical Properties: Determination and Report of Procedures,"*2012.

35. *ULTEM™ Fibers Resin data sheet*. 2014 [cited 2014 7 May 2014]; Available from: https://www.sabic-ip.com/gepapp/eng/weather/weatherhtml?sltRegionList=1002002000&sltPrd=1002003018&sltGrd=1002017796&sltUnit=0&sltModule=DATASHEETS&sltVersion=Internet&sltType=Online.

9. Appendix A: Materials specifications

Table 10. ULTEM ™ Film Resin 1000 materials data sheet [5]

MECHANICAL	Value	Unit	Standard
Tensile Stress, yld, Type I, 5 mm/min	1120	kgf/cm²	ASTM D 638
Tensile Strain, yld, Type I, 5 mm/min	7	%	ASTM D 638
Tensile Strain, brk, Type I, 5 mm/min	60	%	ASTM D 638
Tensile Modulus, 5 mm/min	36500	kgf/cm²	ASTM D 638
Flexural Stress, yld, 2.6 mm/min, 100 mm span	1680	kgf/cm²	ASTM D 790
Flexural Modulus, 2.6 mm/min, 100 mm span	35800	kgf/cm²	ASTM D 790
Hardness, Rockwell M	109	-	ASTM D 785
Taber Abrasion, CS-17, 1 kg	10	mg/1000cy	ASTM D 1044
IMPACT			
Izod Impact, unnotched, 23°C	136	cm-kgf/cm	ASTM D 4812
Izod Impact, notched, 23°C	5	cm-kgf/cm	ASTM D 256
Izod Impact, Reverse Notched, 3.2 mm	136	cm-kgf/cm	ASTM D 256
Gardner, 23°C	373	cm-kgf	ASTM D 3029
THERMAL			
Vicat Softening Temp, Rate B/50	218	°C	ASTM D 1525
HDT, 0.45 MPa, 6.4 mm, unannealed	210	°C	ASTM D 648
HDT, 1.82 MPa, 6.4 mm, unannealed	201	°C	ASTM D 648
CTE, -20°C to 150°C, flow	5.58E-05	1/°C	ASTM E 831
CTE, -20°C to 150°C, xflow	5.4E-05	1/°C	ASTM E 831
Thermal Conductivity	0.22	W/m-°C	ASTM C 177
Relative Temp Index, Elec	170	°C	UL 746B
PHYSICAL			
Specific Gravity	1.27	-	ASTM D 792
Water Absorption, 24 hours	0.25	%	ASTM D 570
Water Absorption, equilibrium, 23C	1.25	%	ASTM D 570
Mold Shrinkage, flow, 3.2 mm (5)	0.5 - 0.7	%	SABIC Method
Melt Flow Rate, 337°C/6.6 kgf	9	g/10 min	ASTM D 1238
FLAME CHARACTERISTICS			
UL Recognized, 94V-2 Flame Class Rating (3)	0.4	mm	UL 94
UL Recognized, 94V-0 Flame Class Rating (3)	0.75	mm	UL 94
UL Recognized, 94-5VA Rating (3)	3	mm	UL 94
Oxygen Index (LOI)	47	%	ASTM D 2863
NBS Smoke Density, Flaming, Ds 4 min	0.7	-	ASTM E 662

Table 11. ULTEM ™ fibers Resin 9011 materials data sheet [35]

MECHANICAL	Value	Unit	Standard
Tensile Stress, yld, Type I, 5 mm/min	**1120**	**kgf/cm²**	**ASTM D 638**
Tensile Stress, brk, Type I, 5 mm/min	1070	kgf/cm²	ASTM D 638
Tensile Strain, yld, Type I, 5 mm/min	**7**	**%**	**ASTM D 638**
Tensile Strain, brk, Type I, 5 mm/min	60	%	ASTM D 638
Tensile Modulus, 5 mm/min	**36600**	**kgf/cm²**	**ASTM D 638**
Flexural Stress, yld, 1.3 mm/min, 50 mm span	1680	kgf/cm²	ASTM D 790
Flexural Modulus, 1.3 mm/min, 50 mm span	**35800**	**kgf/cm²**	**ASTM D 790**
Tensile Stress, yield, 5 mm/min	105	MPa	ISO 527
Tensile Stress, break, 5 mm/min	**85**	**MPa**	**ISO 527**
Tensile Strain, yield, 5 mm/min	6	%	ISO 527
Tensile Strain, break, 5 mm/min	**60**	**%**	**ISO 527**
Tensile Modulus, 1 mm/min	3200	MPa	ISO 527
Flexural Stress, yield, 2 mm/min	**160**	**MPa**	**ISO 178**
Flexural Modulus, 2 mm/min	3300	MPa	ISO 178
IMPACT			
Izod Impact, unnotched, 23°C	136	cm-kgf/cm	ASTM D 4812
Izod Impact, notched, 23°C	**3**	**cm-kgf/cm**	**ASTM D 256**
Izod Impact, notched, -30°C	3	cm-kgf/cm	ASTM D 256
Izod Impact, Reverse Notched, 3.2 mm	**119**	**cm-kgf/cm**	**ASTM D 256**
Instrumented Impact Total Energy, 23°C	336	cm-kgf	ASTM D 3763
Izod Impact, unnotched 80*10*4 +23°C	**NB**	**kJ/m²**	**ISO 180/1U**
Izod Impact, unnotched 80*10*4 -30°C	NB	kJ/m²	ISO 180/1U
Izod Impact, notched 80*10*4 +23°C	**5**	**kJ/m²**	**ISO 180/1A**
Izod Impact, notched 80*10*4 -30°C	5	kJ/m²	ISO 180/1A
Charpy 23°C, V-notch Edgew 80*10*4 sp=62mm	**3**	**kJ/m²**	**ISO 179/1eA**
THERMAL			
Vicat Softening Temp, Rate B/50	**219**	**°C**	**ASTM D 1525**
HDT, 0.45 MPa, 3.2 mm, unannealed	205	°C	ASTM D 648
HDT, 1.82 MPa, 3.2mm, unannealed	**197**	**°C**	**ASTM D 648**
HDT, 0.45 MPa, 6.4 mm, unannealed	207	°C	ASTM D 648
HDT, 1.82 MPa, 6.4 mm, unannealed	**199**	**°C**	**ASTM D 648**
CTE, -40°C to 150°C, flow	5.50E-05	1/°C	ASTM E 831
CTE, -40°C to 150°C, xflow	**5.50E-05**	**1/°C**	**ASTM E 831**
CTE, 23°C to 150°C, flow	5.00E-05	1/°C	ISO 11359-2
CTE, 23°C to 150°C, xflow	**5.00E-05**	**1/°C**	**ISO 11359-2**
Ball Pressure Test, 125°C +/- 2°C	Passes	-	IEC 60695-10-2
Vicat Softening Temp, Rate A/50	**215**	**°C**	**ISO 306**
Vicat Softening Temp, Rate B/50	211	°C	ISO 306
Vicat Softening Temp, Rate B/120	**212**	**°C**	**ISO 306**
HDT/Be, 0.45MPa Edgew 120*10*4 sp=100mm	200	°C	ISO 75/Be
HDT/Ae, 1.8 MPa Edgew 120*10*4 sp=100mm	**190**	**°C**	**ISO 75/Ae**
HDT/Af, 1.8 MPa Flatw 80*10*4 sp=64mm	193	°C	ISO 75/Af

Table 8 (continued)

PHYSICAL	Value	Unit	Standard
Specific Gravity	1.27	-	ASTM D 792
Mold Shrinkage on Tensile Bar, flow (2) (5)	**0.5 - 0.7**	**%**	**SABIC Method**
Mold Shrinkage, flow, 3.2 mm (5)	0.5 - 0.7	%	SABIC Method
Mold Shrinkage, xflow, 3.2 mm (5)	**0.5 - 0.7**	**%**	**SABIC Method**
Melt Flow Rate, 337°C/6.6 kgf	17.8	g/10 min	ASTM D 1238
Density	**1.27**	**g/cm³**	**ISO 1183**
Water Absorption, (23°C/sat)	1.25	%	ISO 62
Moisture Absorption (23°C / 50% RH)	**0.7**	**%**	**ISO 62**
Melt Volume Rate, MVR at 360°C/5.0 kg	25	cm³/10 min	ISO 1133
FLAME CHARACTERISTICS			
Oxygen Index (LOI)	44	%	ASTM D 2863

Typical Fiber Properties		Inch-Pound	SI
Tensile strength	3K E13 (EP03)	610 ksi	4205 MPa
	6K E13	630 ksi	4345 MPa
	12K E13	620 ksi	4275 MPa
	12K/24K F13 (F301)	670 ksi	4620 MPa
Tensile modulus*	3K/6K/12K E13 [1]	34.3 Msi	237 GPa
	12K/24K F13 [2]	34.7 Msi	239 GPa
Elongation*	3K E13 [1]	1.78%	
	6K E13 [1]	1.82%	
	12K E13 [1]	1.80%	
	12K/24K F13 [2]	1.80%	
Density		0.064 lb/in³	1.76 g/cc
Yield/Linear density (with sizing)	3K E13 (EP03)	2456 yd/lb	202 tex (g/km)
	6K E13	1222 yd/lb	406 tex
	12K E13	612 yd/lb	810 tex
	12K F13 (F301)	620 yd/lb	800 tex
	24K F13	310 yd/lb	1600 tex
Sizing level w/w	3K/6K/12K E13 (EP03)	1.30%	
	12K/24K F13 (F301)	1.00%	
Yarn / Tow Characteristics			
Filament Diameter		7.0 x 10^{-6} m	
Twist		Never Twisted	
Equivalent Yarn Cross Section	3K	1.79 x 10^{-4} in² (0.115 mm²) Nominal	
	6K	3.58 x 10^{-4} in² (0.231 mm²) Nominal	
	12K	7.16 x 10^{-4} in² (0.462 mm²) Nominal	
	24K	1.43 x 10^{-4} in² (0.924 mm²) Nominal	

* Toho Tenax Impregnated Strand Test Method. Based on [1] JIS R7601 or [2] DIN 29965

Figure 35. Properties of 3K Tenax®- J HTS40 carbon fibers grade.

10. Appendix B: Test Results

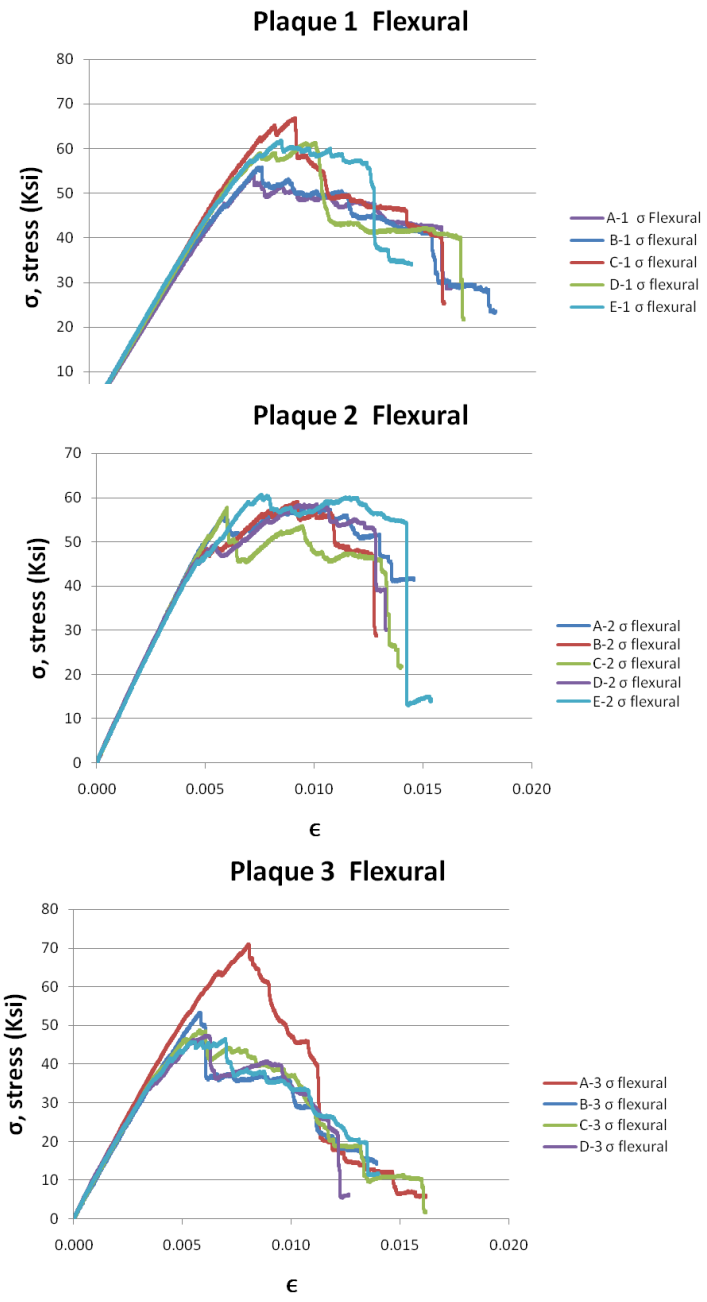

Figure 36. Flexural stress–strain curves of co-mingled specimens.

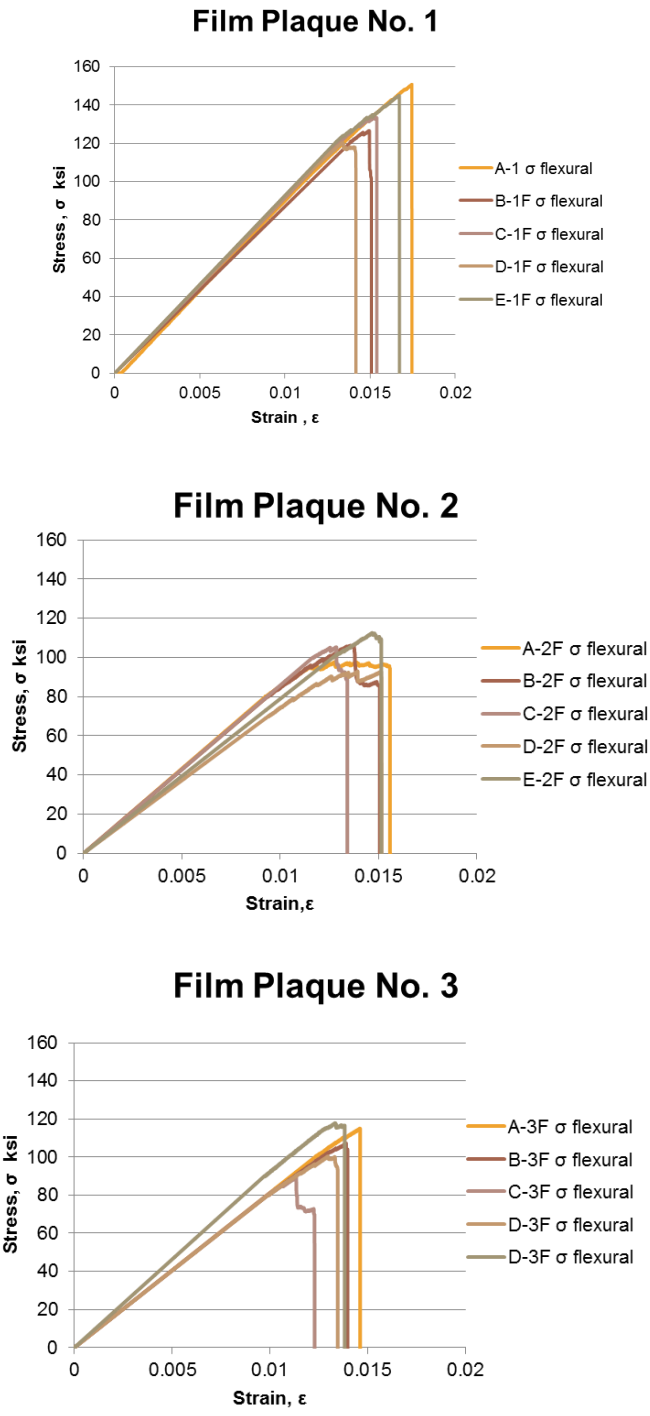

Figure 37. Flexural stress–strain curves of film specimens.

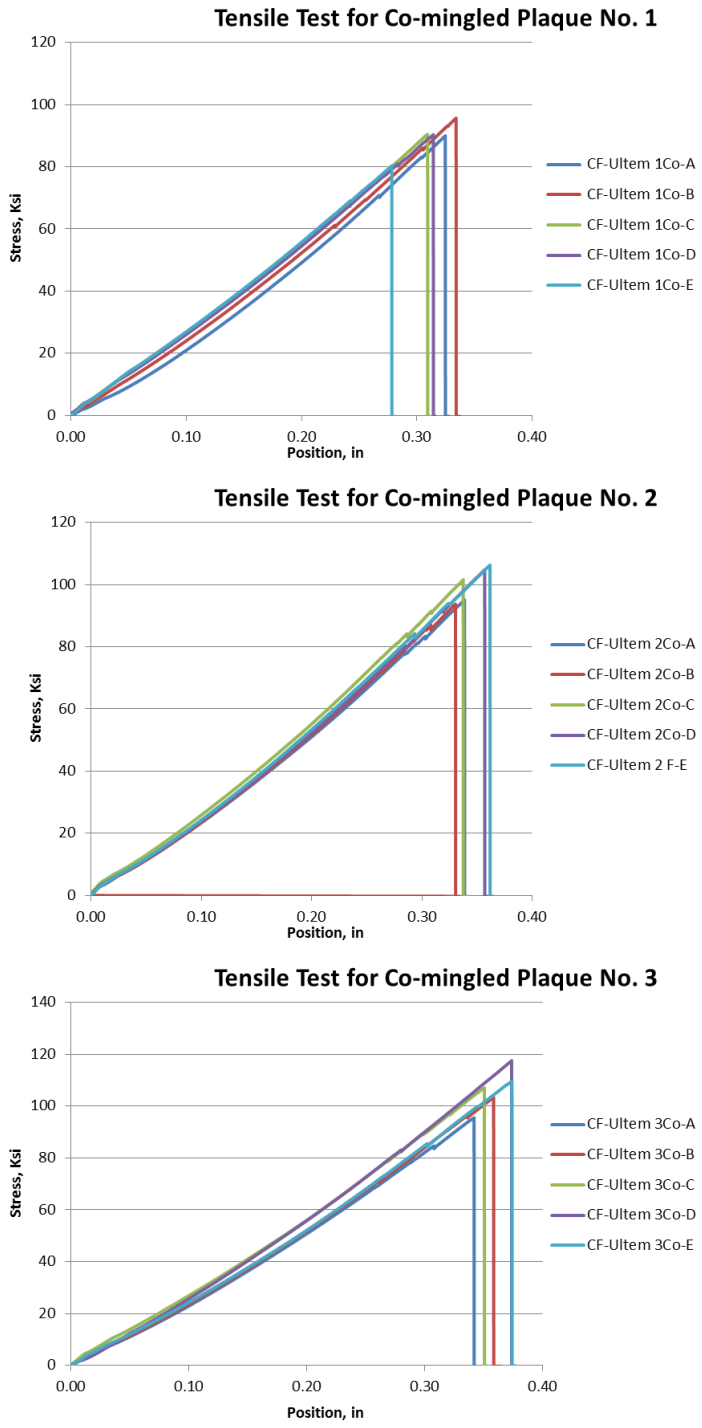

Figure 38. Tensile stress–displacement curve for co-mingled specimens.

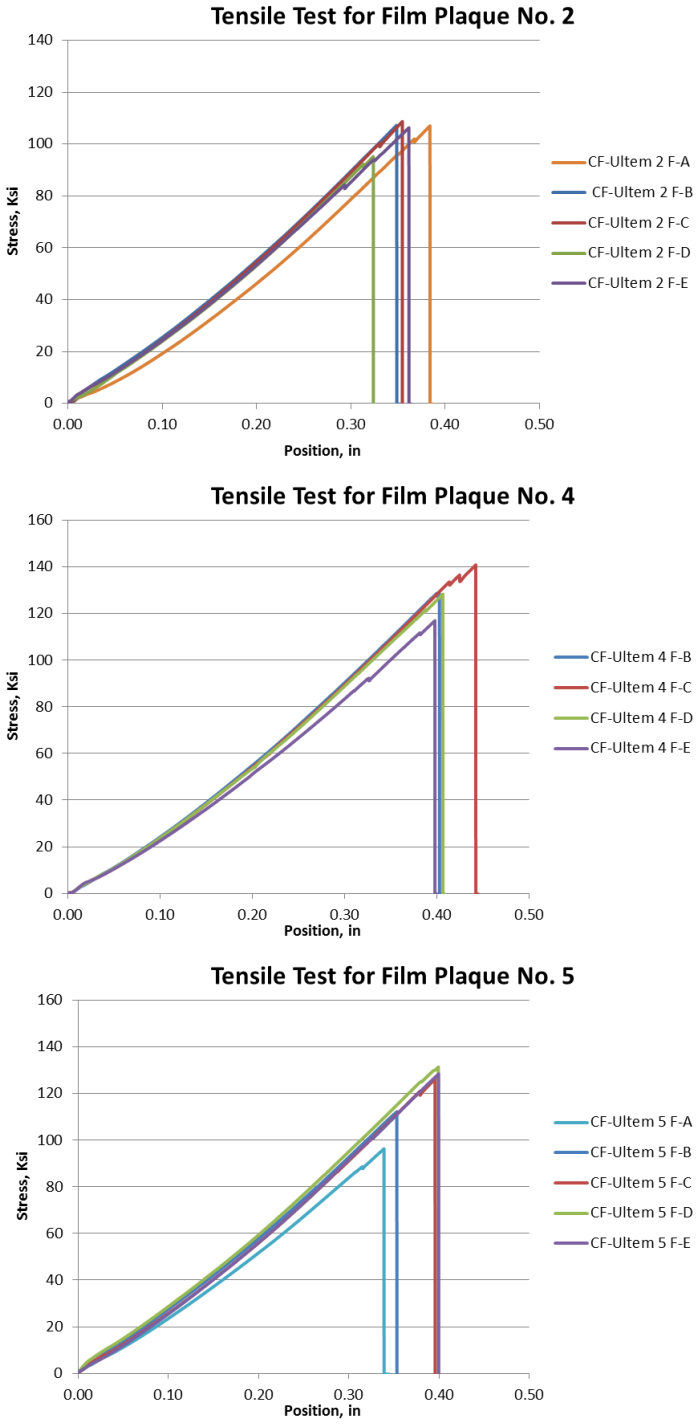

Figure 39. Tensile stress–displacement curves for film specimens.

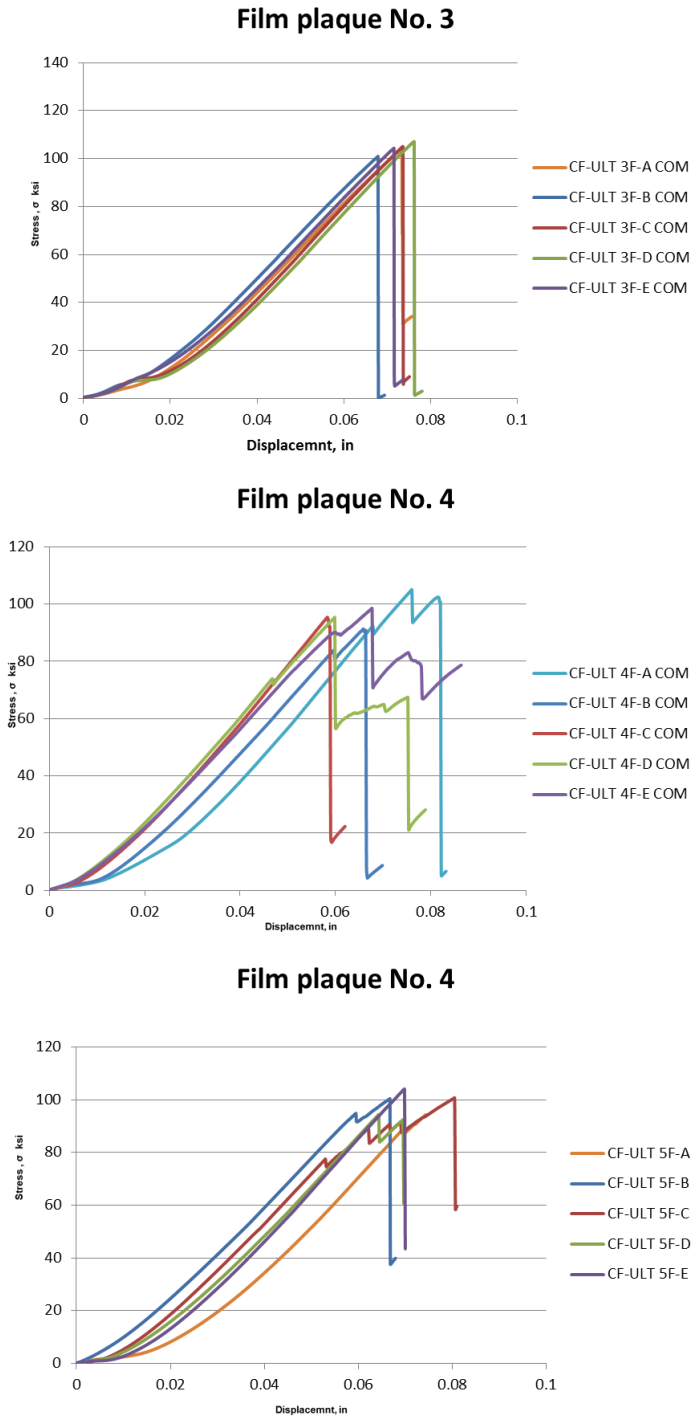

Figure 40. Compression stress–displacement curves for film specimens.

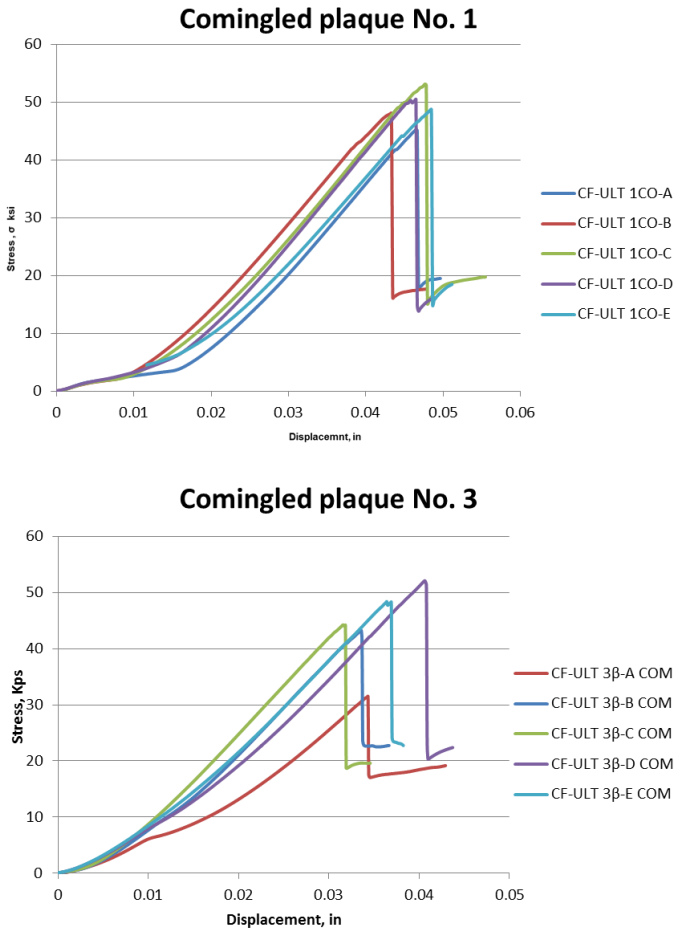

Figure 41. Compression stress–displacement curves for co-mingled specimens.

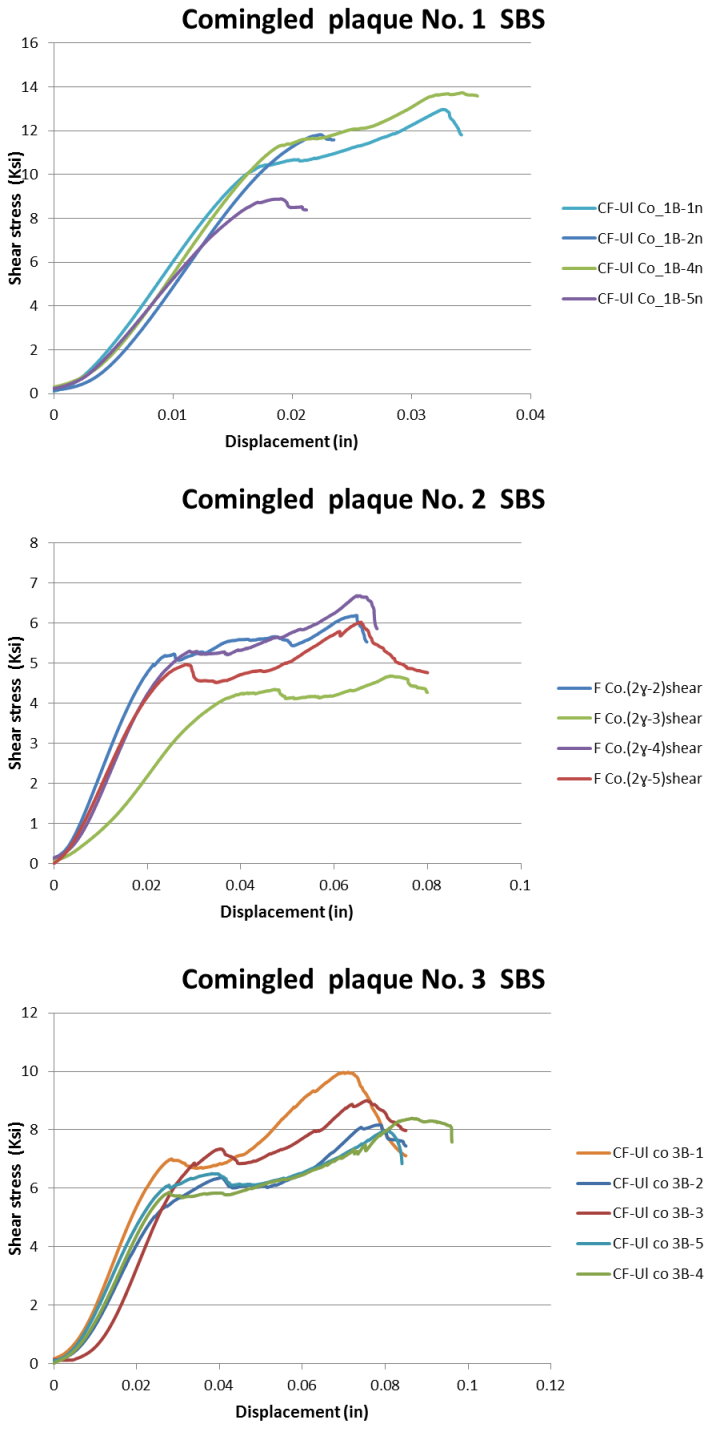

Figure 42. SBS stress–displacement curves for co-mingled specimens.

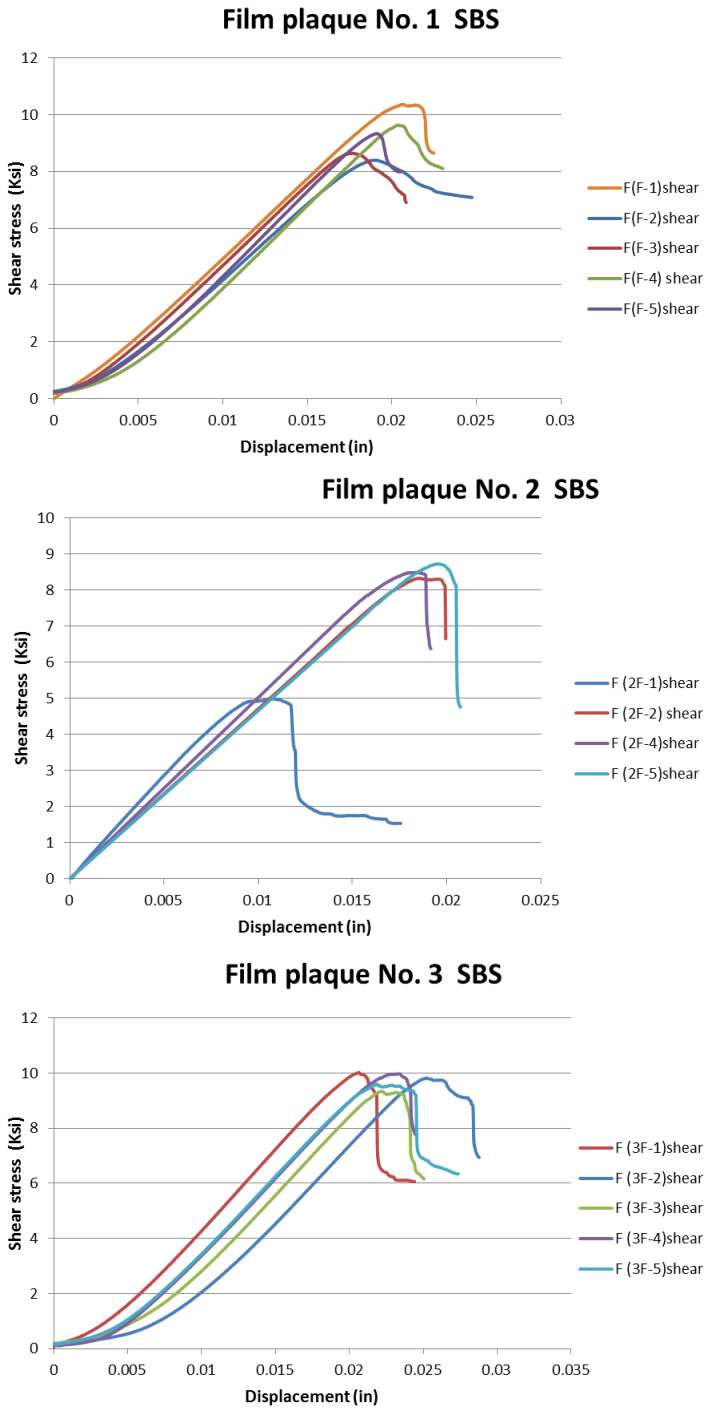

Figure 43. SBS stress–displacement curves for film specimens.

11. Appendix C: Microscopic Pictures.

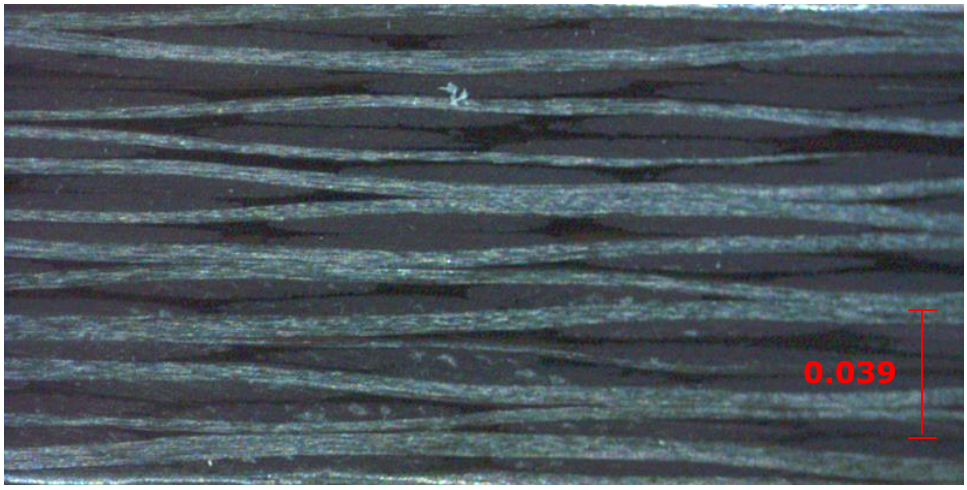

Figure 44. Optical microscopic cross-section image for CF/PEI film specimen.

Figure 45. Optical microscopic cross-section image for CF/PEI co-mingled specimen.

Table 12 Key name labeling for CF/PEI film and co-mingle plaques

Plaque No.	Description
F-1	CF/PEI Film plaque No. 1
F-2	CF/PEI Film plaque No. 2
F-3	CF/PEI Film plaque No. 3
F-4	CF/PEI Film plaque No. 4
F-5	CF/PEI Film plaque No. 5
Co-1	CF/PEI Co-mingle plaque No. 1
Co-2	CF/PEI Co-mingle plaque No. 2